Analytic theory for parity breaking in lamellar eutectic growth

Alexandre Valance,* Chaouqi Misbah, and Dmitrii Temkin†
Institut Laue Langevin, Boîte Postale 156X, 38042 Grenoble CEDEX, France

Klaus Kassner
Institut für Festkörperforschung des Forschungszentrums Jülich, W-517 Jülich, Germany
(Received 24 May 1993)

An extensive analytic analysis of tilted lamellar growth is presented. We first confine ourselves to a situation where both solid phases are identical and the concentration is maintained at the eutectic composition far ahead of the solidification front. A Rapid Communication has already been devoted to this case [C. Misbah and D. E. Temkin, Phys. Rev. A **46**, R4497 (1992)]. Here, we first focus on an extensive analysis of this problem and a comparison with the full numerical calculation. We find good agreement between the two situations, a fact which confers confidence in the applicability of our analytic results to real situations. In the second line of this work, we shall analyze the effect of an off-eutectic composition. We show, contrary to some previous work based on a random-walker method, that the effect of the homogeneous boundary layer (which plays the role of a total net charge in an electrostatic analogy) does not play a crucial role for parity breaking, in agreement with our previous numerical work in the continuous limit. Finally, the effect of crystalline anisotropy is analyzed. It is shown that the bifurcation equation, which is of pitchfork type in the isotropic case, becomes imperfect.

PACS number(s): 61.50.Cj, 05.70.Fh, 81.30.Fb, 68.70.+w

I. INTRODUCTION

It is well known that when a eutectic alloy is submitted to directional solidification—that is by pulling the sample at a constant speed in an external thermal gradient—the solid often exhibits a steady and spatially organized structure consisting of a periodic array of alternating lamellae of the two solid phases α and β: the two phases grow in a cooperative manner, a growth which is essentially limited by interlamellar diffusion of the two substances of the alloy. A seminal theoretical paper was given by Jackson and Hunt (JH) [1]. The crucial point of their theory was to replace, in a first step, the actual front (which is an unknown quantity of the problem; a free boundary problem) by that of a planar front on the average. This allowed them to compute the diffusion field in the liquid phase, which is compatible with mass conservation. They then render the problem self-consistent by imposing to the computed field to satisfy local chemical equilibrium (appropriate for a molecularly rough interface),—or the Gibbs-Thomson condition. Emerging from this is a relationship between the average front undercooling Δ and the wavelength of the pattern λ. This result can be inferred from a simple argument. Indeed, the growth velocity is, from purely dimensional analysis, given by D/λ and the proportionality coefficient is (up to a multiplicative number) the dimensionless supersaturation (see Fig. 1), $V \sim \Delta D/\lambda$ (the linear dependence on Δ stems from linear thermodynamics). On the other hand, the growth can occur only if the wavelength of the pattern is typically larger than the nucleation radius, approximately given by λ_c/Δ, where λ_c is of the order of the capillary length, so that the growth velocity takes the form

$$V \sim \frac{D\Delta}{\lambda} \left[1 - \frac{\lambda_c}{\Delta\lambda} \right] . \tag{1.1}$$

This is—besides small details—the important result that follows from the JH calculation. In directional solidification, the growth speed V is fixed while the unknown quantity is the front undercooling Δ (which is a measure of the average front position in the applied thermal gradient). This quantity is given from Eq. (1.1) by

$$\Delta \sim \frac{V}{D}\lambda + \frac{\lambda_c}{\lambda} . \tag{1.2}$$

The first term represents the diffusion effect while the second one the capillary contribution. Figure 2 shows Δ as a function of λ, which takes on a minimum at a typical wavelength $\lambda_{min} \sim 1/\sqrt{V}$. This wavelength plays an important role and has often been considered as the natural wavelength which is selected by the physical system [2].

Since JH a considerable amount of work has been devoted to the theory of lamellar eutectics, for which we have given a brief account in the introduction of a recent paper [3]. It is now well established that the JH curve (Fig. 2) should be modified to include the following features, discovered by solving the full growth equations [3–5]. (i) For a given λ there exists a discrete set of solutions characterized by their average undercooling (Fig. 3) and not a unique solution as in the JH equation; i.e., we have many branches $\Delta(\lambda)$. (ii) When typically $\lambda \simeq 2\lambda_{min}$, the branches coalesce by pairs to form *fold singularities*, above which steady-state symmetric solutions cease to exist. (iii) Slightly before the *fold* singularities take place, two new branches emerge as a forward bifurcation: the
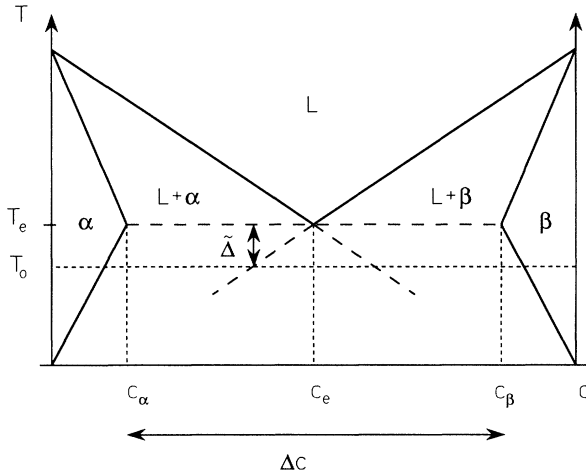
FIG. 1. Schematic phase diagram of a eutectic alloy. T is the temperature and c the concentration of one component. The regions L, α, and β correspond to one-phase equilibrium states of the liquid, the solid α, and the solid β phases, respectively. $L + \alpha$ and $L + \beta$ are regions of two-phase equilibrium between the liquid and one solid phase; the true concentrations of the two phases are given by the liquidus and solidus lines (full lines) delimiting these regions. c_e, c_α, and c_β denote the equilibrium concentrations of the liquid and the two solid phases at the eutectic point, whose temperature is T_e. Δc is the miscibility gap: $\Delta c = c_\beta - c_\alpha$. Finally, $\tilde{\Delta}$ is the undercooling (measured in physical unit): $\tilde{\Delta} = T_e - T_0$ where T_0 is the melt temperature.

FIG. 3. Average undercooling as a function of λ for four branches of axisymmetric solutions to the full growth equations (squares, tip-down and tip-up triangles, and circles). The symmetric branches form two pairs, whose members coalesce into fold singularities at a critical wavelength λ_c. For $\lambda > \lambda_c$, no axisymmetric solutions exist. Slightly before the fold, two new branches merge as forward bifurcations.

lower one corresponds to global parity breaking where both lamellae cooperate and the upper one to a situation where the two lamellae act against each other for the choice of the sign of the antisymmetric component (each lamellae chooses a different direction, and the widest one wins). In particular, when both lamellae have exactly the same properties, the upper branch would correspond to a situation where each of them is asymmetric but a mirror image of the other; as a consequence the pattern is not traveling anymore.

The parity-breaking bifurcation is a robust feature met experimentally in many physical situations [6–8] and dealt with theoretically in different contexts [9–13]. Ex-
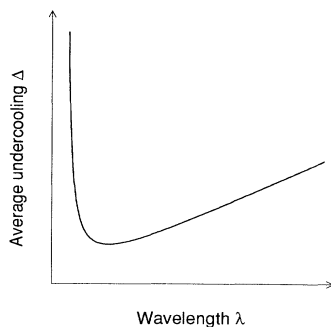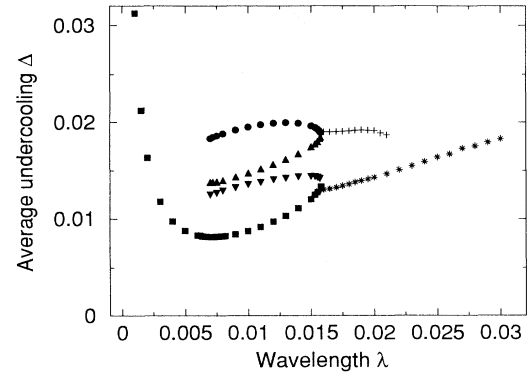
cept in the situation where the dynamics can be mapped onto that of two coupled Fourier modes—a situation met close to the codimension-two bifurcation—most of the progress first came from numerical works. In particular, the eutectic system seemed to defy an analytic treatment. We found [4] that the JH theory, although it misses the various features described above, describes remarkably well the symmetric pattern below the *fold*. In particular, this also holds close enough to the birth of the broken-parity state. This gave us a strong hint that a simple treatment, similar to that of JH, which involves an antisymmetric component in the front profile should constitute a good starting point for the analytic theory of parity breaking. We have indeed built up an analytic theory which has captured the essential features and to which we have already [11] devoted a Rapid Communication. The main purpose of the present paper is threefold.

First we shall give an extensive analysis of the parity-breaking bifurcation for a completely symmetric system–that is, in a situation where the two solid phases have identical properties—and with the concentration far ahead of the solidification front maintained at the eutectic composition. We make a comparison with the full numerical analysis. We find good agreement between the two treatments. This gives confidence to our analytic work, in the utilization of our analytic expression for experiments.

Second, we shall relax the condition that the concentration is at the eutectic composition, while keeping all the other properties identical. This part is motivated by a belief that the deviation from eutectic compositions plays the role of a sort of a driving force for some instabilities, such as the oscillatory [14] instability and the tilting one [15]. This has naturally led us to elucidate this question and to see whether the tilting instability, for example, necessitates an off-eutectic composition or not. In our previous numerical analysis [5], we did not find that being at the eutectic point is crucial for parity breaking, a result which has been corroborated by recent Monte Car-

FIG. 2. Δ as a function of λ obtained from the Jackson-Hunt theory.

lo simulations [16]. It is instructive to investigate in our analytic treatment how the off-eutectic composition enters the parity-breaking bifurcation. We have elucidated this question. First we should note that being at an off-eutectic composition results in a homogeneous diffusion layer ahead of the front. In an electrostatic analogy, this means that there is a total net charge, creating a Yukawa-like potential, in addition to the dipolarlike distribution (since one phase absorbs, say the B component of the alloy, while the other one rejects it, there is a pluslike-negativelike charge distribution—a dipolar distribution). Our analytic analysis shows that the homogeneous layer does not enter directly the parity-breaking mechanism (it enters just in the global mass conservation—an obvious effect). In other words, the mechanism is, in some sense, a "screening" effect of dipoles in the mechanism of parity breaking. This statement should not mean that the effect of the "total charge" is completely absent in eutectic growth, but only that it is unimportant for antisymmetric fluctuations. Another way of viewing this is to realize that, to leading order, an off-eutectic composition creates only a symmetric component in the diffusion field to which parity breaking is indifferent.

The third line of the paper has its source in experimental observations according to which the crystalline anisotropy, although weak, plays a crucial role in the dynamics of tilted domains. In recent work we have investigated numerically and phenomenologically the role of anisotropy. Here we shall show analytically from the "microscopic" model, that the coupling between the spontaneous parity-breaking bifurcation and the crystalline anisotropy destroys the pitchfork bifurcation in favor of an imperfect one.

The scheme of this paper is as follows. In Sec. II we write down the basic equations. In Sec. III we deal with the theory of spontaneous tilted growth. We first examine the case of symmetric systems and we compare the results with those obtained from the full numerical calculation. Then we extend the calculation to the off-eutectic systems. In Sec. IV we analyze the effect of crystalline anisotropy. The conclusion and outlook are presented in Sec. V. Some technical details are relegated to three appendixes.

II. BASIC EQUATIONS

Since the model equations have been already described in detail in our previous work [4], we will keep their discussion brief. For the moment, we neglect surface tension anisotropy. In Sec. IV we shall make the changes implied by anisotropy.

Let c be the concentration in the liquid of one of the components of the eutectic system, c_e its value at the eutectic point, and Δc the miscibility gap—see the phase diagram given in Fig. 1. In terms of the dimensionless concentration field $u = (c - c_e)/\Delta c$, the diffusion equation for a tilted pattern with a tilt angle ϕ reads

$$\frac{1}{D}\frac{\partial u}{\partial t} = \nabla^2 u + \frac{2}{l}\left[\frac{\partial u}{\partial z} + \tan(\phi)\frac{\partial u}{\partial x}\right] . \quad (2.1)$$

Coordinates are measured in a frame of reference that is attached to the liquid-solid interface (and is identical to the laboratory frame for $\phi = 0$). In this equation, D is the diffusion coefficient, $l = 2D/V$ is the diffusion length, and V is the pulling velocity. If the tilt angle is nonzero, the interface moves, in the laboratory frame, with a velocity $V\tan(\phi)$ along the x direction. Equation (2.1) is subject to the condition far ahead of the solidification front

$$u(z = \infty) \equiv u_\infty = (c_\infty - c_e)/\Delta c , \quad (2.2)$$

where u_∞ may be positive (hypereutectic), negative (hypoeutectic), or zero (eutectic), and to mass conservation at the liquid-solid interface $[z = \zeta(x,t)]$

$$-D\frac{\partial u}{\partial n}\bigg|_{\text{interface}} = \begin{cases} +v_n/2, & \alpha \text{ phase} \\ -v_n/2, & \beta \text{ phase} , \end{cases} \quad (2.3)$$

where $v_n = (V + \dot{\zeta})n_z + V\tan(\phi)n_x$ is the normal velocity of the interface. The normal vector $\mathbf{n}$ points from the solid to the liquid. Note that use has been made of the fact that the two solid phases are equivalent [i.e., $(c_e - c_\alpha)/\Delta c = \frac{1}{2}$ and $(c_e - c_\beta)/\Delta c = -\frac{1}{2}$]. Furthermore the partition coefficients k_α and k_β have been taken to be equal to 1. Finally, for a molecularly rough liquid-solid interface chemical equilibrium results in the Gibbs-Thomson condition at the two boundaries

$$u\big|_{\text{interface}} = \begin{cases} -\zeta/l_T - d_0\kappa, & \alpha \text{ phase} \\ \zeta/l_T + d_0\kappa, & \beta \text{ phase} , \end{cases} \quad (2.4)$$

where

$$l_T = \frac{m_l \Delta c}{G}, \quad d_0 = \frac{\gamma_{sl} T_e}{L m_l \Delta c} \quad (2.5)$$

are the thermal and the capillary lengths, respectively, κ is the front curvature taken positive where the solid is convex, m_l is the modulus of the slope of the liquidus lines, γ_{sl} is the liquid-solid interface tension, and L is the latent heat per unit volume. Since the two solid phases α and β are taken to be equivalent, the three quantities m_l, γ_{sl}, and L characterize the liquid-solid α transition as well as the liquid-solid β one.

Let us make a few remarks about Eq. (2.4). First, the capillary length has been defined here in the pure isotropic case (the surface tension γ_{sl} has been taken independent of the liquid-solid interface orientation). In the presence of crystalline anisotropy the surface tension should be replaced by the surface stiffness, as we will see in Sec. IV. Second, for our practical purpose, we will approximate ζ/l_T by $\langle\zeta\rangle/l_T$, which means that the front can be viewed to be, practically, in an isothermal environment. This is justified by the fact that the front excursion, which is of order λ, is much smaller than the thermal length (in standard experiments, $l_T/l \sim 1$ while $\lambda/l \sim 10^{-2}$). Note that $-\langle\zeta\rangle/l_T$ is nothing but the dimensionless average front undercooling Δ ($\Delta = \langle T_e - T_i\rangle/m_l\Delta c$ where T_i is the temperature of the interface).

Finally, to complete our set of equations we impose mechanical equilibrium at the triple point, where the

three phases meet

$$\gamma_{\alpha\beta} + \gamma_{\alpha l} + \gamma_{\beta l} = 0 \ . \tag{2.6}$$

The vector γ_{ij} designates the surface tension between phase i and phase j. If the surface tensions are known, then Eq. (2.6) determines uniquely the contact angle for axisymmetric lamellae (see Fig. 4). We shall denote by θ this contact angle. For a tilted pattern with a tilt angle ϕ, the angles between the tangents at the liquid-α,β intersection and the horizontal axis (see Fig. 4) at two ends of a given lamella are different (because of asymmetry). Let $\tilde{\theta}$ and $\tilde{\theta}'$ denote these two angles, either for the α phase or the β phase. It is easy to see from Fig. 4 that

$$\tilde{\theta} = \theta - \phi, \quad \tilde{\theta}' = \theta + \phi \ . \tag{2.7}$$

The set of equations (2.1)–(2.7) completely describes the solidification dynamics.

III. PARITY BREAKING

In this section we deal with the analytic treatment for parity breaking. We examine first the case where the melt is exactly at the eutectic composition (i.e., $u_\infty = 0$). Because the treatment in this case is much simpler than in the general situation, it is instructive to begin with, in order to easily identify the main physical ingredients. Before going further we rewrite the basic equations in dimensionless form. For that purpose, we take the diffusion length l as a unit. For a stationary tilted pattern, Eq. (2.1) takes the form

$$\nabla^2 u + 2u_z + 2\tan(\phi)u_z = 0 \ , \tag{3.1}$$

subject to mass conservation and Gibbs-Thomson conditions at the interface $[z = \zeta(x)]$

$$u_z - \zeta_x u_x = \mp [1 - \zeta_x \tan(\phi)] \ , \tag{3.2}$$

$$u = \pm(\Delta - d_0\kappa) \ . \tag{3.3}$$

The upper and the lower signs refer to the solid α phase and the β phase, respectively. Finally the mechanical equilibrium conditions at the triple points can be rewritten as

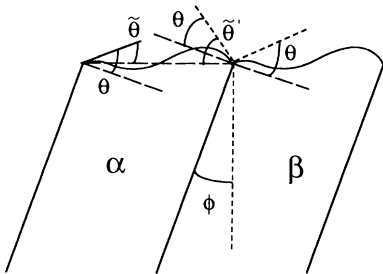$$\zeta_x(0) = \tan(\theta - \phi), \quad \zeta_x(x_e) = -\tan(\theta + \phi) \tag{3.4}$$

for the α lamella and

$$\zeta_x(x_e) = \tan(\theta - \phi), \quad \zeta_x(\lambda) = -\tan(\theta + \phi) \tag{3.5}$$

for the β lamella. The quantity x_e designates the x position of the triple point.

A. Euctectic compositions

We consider here the completely symmetric case ($u_\infty = 0$). As a consequence of mass conservation, the lamellar growth structure has the following feature: the two lamellae α and β have exactly the same width (the volume fraction η of the α phase is equal to $\frac{1}{2}$).

The spirit of the calculation is inspired by that of JH for axisymmetric states [1]. To determine the diffusion field for axisymmetric states, JH assume that the front is planar, sitting at an average position, which is *a priori* unknown. That is, they solve Eq. (3.1) subject to condition (3.2) at $\zeta = \bar{\zeta}$, $u_z(\bar{\zeta}) = \mp 1$. Using the expression of this diffusion field at $z = \bar{\zeta}$, the Gibbs-Thomson equation provides an ordinary second-order differential equation for the interface position $\zeta(x)$, which can be solved, in principle, or directly averaged. Emerging from this analysis is a relationship between the front undercooling and λ [basically Eq. (1.2)].

The simplest treatment beyond that of JH involving broken-parity solutions consists in solving the von Neumann problem [i.e., Eq. (3.1) subject to the boundary condition Eq. (3.2)] by considering a small asymmetric deviation from the planar interface. The profile is taken as simple as

$$\zeta(x) - \bar{\zeta} = \begin{cases} x\tan(\theta - \phi), & 0 \leq x \leq x_0 \tag{3.6} \\ (\lambda/2 - x)\tan(\theta + \phi), & x_0 \leq x \leq \lambda/2 \tag{3.7} \end{cases}$$

where x_0 is the intersection point (see Fig. 5), given by $x_0 = \lambda \tan(\theta + \phi)/2[\tan(\theta + \phi) + \tan(\theta - \phi)]$.

The first step is to determine the diffusion field corresponding to the front defined above. We write the gen-

FIG. 4. Definition of the contact angle θ, the pinning angles $\tilde{\theta}$ and θ', and the tilt angle ϕ. Note that ϕ is counted positive for a tilt to the right, while θ is always positive.
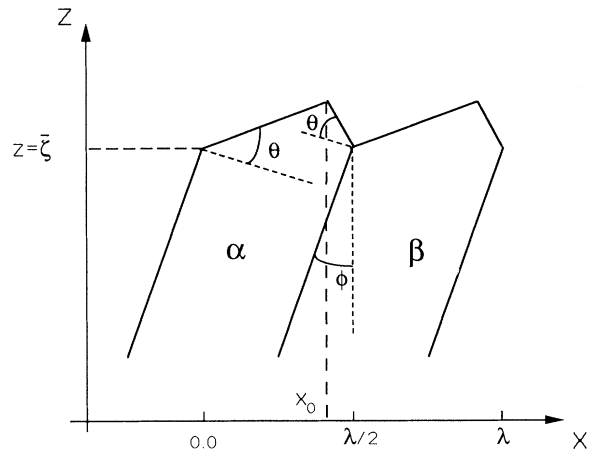

FIG. 5. The front profile used to determine the diffusion field for a completely symmetric system.

eral solution of the stationary diffusion equation [Eq. (3.1)] for a spatially periodic system as

$$u(x,z) = \sum_n C_n e^{ik_n x} e^{-Q_n(z-\bar\xi)} , \qquad (3.8)$$

where $k_n = 2\pi n/\lambda$, $Q_n = 1 + \sqrt{1 + k_n^2 - 2ik_n\tan(\phi)}$, and C_n are undetermined coefficients for the moment. In the (standard) small-Péclet-number (which is just λ in reduced units) limit $Q_n \simeq |k_n|$ for $n \neq 0$ ($Q_0 = 2$).

To determine the diffusion field (i.e., the coefficients C_n) to leading order in the deviation from JH theory, we expand the continuity equation in the front deviation $\zeta - \bar\xi$. Since this quantity is of the order of the Péclet number (recall that ζ is rescaled by the diffusion length), the remaining terms would produce higher-order contributions in the Péclet number. To leading order, the continuity equation takes the form

$$u_z = -(\zeta - \bar\xi)u_{zz}^{(0)} + \zeta_x u_x^{(0)} \mp [1 - \zeta_x \tan(\phi)] , \qquad (3.9)$$

where the fields on both sides are understood to be evaluated at $z = \bar\xi$. The quantity $u^{(0)}$ refers to the JH field

given by (for $u_\infty = 0$)

$$u^{(0)}(x,z) = \sum_{n \neq 0} B_n e^{ik_n x} e^{-Q_n(z-\bar\xi)} , \qquad (3.10)$$

where

$$B_n = \frac{4e^{-in\pi\eta}}{\lambda k_n Q_n}\sin(n\pi\eta) . \qquad (3.11)$$

The coefficients C_n are obtained by inserting (3.8) into Eq. (3.9). After lengthy algebra, the final result can be written as follows:

$$u(x,z) = \sum_{n=1}^{\infty} \left\{ D_{2n-1}\sin\left[\frac{2\pi}{\lambda}(2n-1)x\right] \right.$$
$$\left. + E_{2n-1}\cos\left[\frac{2\pi}{\lambda}(2n-1)x\right] \right\}$$
$$\times e^{-Q_n(z-\bar\xi)} , \qquad (3.12)$$

where

$$D_{2n-1} = \frac{2\lambda}{\pi^2(2n-1)^2} + \frac{\lambda\tan(\phi)}{\pi^2(2n-1)^2}\left\{ H^{(-)} + H^{(+)}\cos\left[\frac{2\pi}{\lambda}x_0(2n-1)\right] \right\} + \frac{\lambda\tan(\theta+\phi)\tan(\theta-\phi)}{\pi(2n-1)H^{(+)}}$$
$$-2\lambda H^{(+)}\sum_{m=1}^{\infty}\frac{1-\cos\left[\frac{4\pi}{\lambda}x_0 m\right]}{\pi^3 m[4m^2-(2n-1)^2]} + \lambda H^{(+)}\sum_{m=1}^{n-1}\frac{1-\cos\left[\frac{4\pi}{\lambda}x_0 m\right]}{\pi^3 m^2[2m-(2n-1)]} , \qquad (3.13)$$

$$E_{2n-1} = -\lambda H^{(+)}\tan(\phi)\frac{\sin\left[\frac{2\pi}{\lambda}x_0(2n-1)\right]}{\pi^2(2n-1)^2} - \lambda H^{(+)}\sum_{m=1}^{\infty}\frac{(2n-1)\sin\left[\frac{4\pi}{\lambda}x_0 m\right]}{\pi^3 m^2[4m^2-(2n-1)^2]}$$
$$+ \lambda H^{(+)}\sum_{m=1}^{n-1}\frac{\sin\left[\frac{4\pi}{\lambda}x_0 m\right]}{\pi^3 m^2[2m-(2n-1)]} , \qquad (3.14)$$

where $H^{(\pm)} = \tan(\theta+\phi)\pm\tan(\theta-\phi)$. We can easily check that D_{2n-1} and E_{2n-1} are even and odd analytic functions of ϕ, respectively. Indeed, it suffices to note that in the transformation $(\phi \to -\phi)$, the quantities $H^{(\pm)}$ and x_0 transform into $\pm H^{(\pm)}$ and $\lambda/2 - x_0$, respectively. The symmetry properties of the coefficients D_{2n-1} and E_{2n-1} result from the fact that the diffusion field is invariant under the transformation $[\phi \to -\phi, x \to -(x - \lambda/2)]$.

At this stage, we make the problem self-consistent by imposing that the diffusion field has to be compatible with the Gibbs-Thomson condition. This yields

$$d_0\frac{\zeta_{xx}}{(1+\zeta_x^2)^{3/2}} + \Delta = \pm u(x,z=\bar\xi,\phi) , \qquad (3.15)$$

where u is the diffusion field determined above. We have put ϕ in the argument of the diffusion field to recall that u is parametrized by ϕ.

The problem therefore reduces to solving a nonlinear differential equation for the interface profile. The integration of this second-order equation over a half-period requires the determination of two integration constants, which are furnished by the two boundary conditions Eq. (3.4) on the slope ζ_x at the triplet point. At this stage ϕ is still undetermined. So it seems as if the present problem could be solved for arbitrary values of ϕ, since we have made no assumption on ϕ. This is fortunately not the case. Indeed, given a front profile that solves Eq. (3.15) subject to the mechanical equilibrium condition Eq. (3.4) will not in general ensure that the two ends of the lamella $[\zeta(0)$ and $\zeta(\lambda/2)]$ are at the same height. Therefore, the demand that the solutions be physical is satisfied by requiring that

$$\zeta(\lambda/2,\phi) - \zeta(0,\phi) = 0 , \qquad (3.16)$$

where again we put ϕ explicitly in the argument, for the same reasons we mentioned above. This equation leads

generically to the selection of a discrete set of ϕ values, as we will see later. The self-consistency equation can be thought of as a minimization condition of a free-energy function in a Landau theory of phase transition. The quantity ϕ is the analog of an order parameter in phase transition phenomena.

It can easily be checked that Eq. (3.16) is satisfied for $\phi=0$. Indeed, for $\phi=0$, the diffusion field is axisymmetric with respect to the center of each lamella [see expression (3.12) by taking $\phi=0$ and consequently $x_0=\lambda/4$]. The front profile, solution of Eq. (3.15), is therefore axisymmetric too, so that the condition is automatically satisfied. The interesting point is to investigate whether Eq. (3.16) is satisfied for a nontrivial value of ϕ.

In order to deal with this question, we proceed as follows. We integrate Eq. (3.15) once over x (from 0 to x) and make use of the mechanical equilibrium condition at $x=0$. We get

$$\frac{\zeta_x}{\sqrt{1+\zeta_x^2}} = \sin(\theta-\phi) + \int_0^x \frac{u-\Delta}{d_0} dx \equiv f(x) . \quad (3.17)$$

The slope ζ_x can be expressed as a function of f, and a second integration over a half-period provides

$$\zeta(\lambda/2,\phi) - \zeta(0,\phi) = F(\phi,\lambda,\mu) , \quad (3.18)$$

where

$$F(\phi,\lambda,\mu) = \int_0^{\lambda/2} \frac{f(x)}{\sqrt{1-f^2}} . \quad (3.19)$$

μ stands for the material and control parameters (e.g., d_0, θ, and l). The self-consistency condition (3.16) amounts then to the search of the zeros of the function F

$$F(\phi,\lambda,\mu) = 0 . \quad (3.20)$$

This equation is a general expression for ϕ as a function of the other parameters. Before exploiting it, let us determine the average front undercooling. For that purpose, we average the Gibbs-Thomson equation [Eq. (3.15)] over one period (actually over a half-period, because the two lamellae α and β are identical). The result is

$$\Delta = \frac{2d_0}{\lambda}\{\sin(\theta+\phi)+\sin(\theta-\phi)\} + 2\sum_{n=1}^{\infty} \frac{D_{2n-1}}{\pi(2n-1)} . \quad (3.21)$$

Equations (3.20) and (3.21) are general expressions which determine ϕ and Δ as a function of the other parameters. Before going further, let us examine the symmetry properties of the average front undercooling and the (bifurcation) function F. We can immediately check that $\Delta(-\phi)=\Delta(\phi)$, as it should be. F has also a well-defined parity, $F(-\phi)=-F(\phi)$, but this is not directly visible on its form (the proof is given in Appendix A). Note that the parity of F tells us immediately that the self-consistency relation is always satisfied for axisymmetric states [$F(\phi=0)=0$], as mentioned earlier.

Now we proceed to the analysis of Eqs. (3.20) and (3.21). These are formally nonlinear algebraic equations

which can easily be solved numerically. We shall not, however, use the "brute-force" approach; rather we wish to pursue the analysis analytically. To do so, an assumption is needed: we assume that the contact angle θ is small enough, an assumption which allows us to push the analysis to the end, and it will turn out that the obtained expressions can safely be extrapolated to finite angles.

A central point in the small contact angle limit is that it becomes legitimate to neglect f^2 against 1 in the square root appearing in the expression of F [Eq. (3.19)]. This assumption can be justified as follows. Indeed, an order of magnitude of f can be deduced from the simple case of symmetric growth (i.e., by using the JH diffusion field). We obtain $f \sim \lambda^2/(\pi^3 d_0)$. For $\lambda \sim \lambda_{min}$, where λ_{min} is the JH minimum undercooling wavelength ($\lambda_{min}^2 \simeq \pi^3 d_0 \sin\theta$), $f \sim \sin\theta$. So for small enough θ, f^2 is small as compared to 1. In this limit, F reduces to a simple integral involving a linear superposition of cosine and sine functions, which is easily evaluated. After a simple manipulation, we obtain

$$F(\phi,\lambda,\mu) = \frac{\lambda}{4}\{\sin(\theta-\phi)-\sin(\theta+\phi)\}$$
$$+ \frac{\lambda^2}{2d_0}\sum_{n=1}^{\infty}\frac{E_{2n-1}}{\pi^2(2n-1)^2} . \quad (3.22)$$

Since we are interested in the possibility for the symmetric front to undergo a transition to the broken-parity state, we only need to analyze the self-consistency equation about the bifurcation point. For that purpose, we perform a Taylor expansion of Eq. (3.22) about $\phi=0$. Up to third order in ϕ this expression yields

$$\pi^4(\sigma_c-\sigma)\phi - \frac{\alpha_2}{4\theta^2}\phi^3 = 0 , \quad (3.23)$$

with

$$\sigma \equiv \frac{d_0}{\lambda^2} = \frac{\tilde{d}_0\tilde{l}}{\tilde{\lambda}^2}, \quad \sigma_c \simeq \frac{\alpha_1}{\pi^4} . \quad (3.24)$$

The tildes indicate that the variables are written in physical units. The calculation has involved evaluations of numerical series, some of them have been evaluated exactly, the others computed numerically. The coefficients α_1 and α_2 are precisely numerical constants obtained from series summation ($\alpha_1=0.66$ and $\alpha_2=2.95$).

Equation (3.23) shows that for $\sigma > \sigma_c$, $\phi=0$ is the only solution, while for $\sigma < \sigma_c$ there exists two solutions in addition to the trivial one, given by

$$\phi = \pm\frac{2\pi^2\theta}{\alpha_2^{1/2}}\sqrt{\sigma_c-\sigma} . \quad (3.25)$$

This result can be interpreted as follows: the axisymmetric solutions undergo a spontaneous supercritical transition to broken-parity states at $\sigma=\sigma_c$. Stated in another way, for a given growth velocity the initially symmetric structure loses its stability in favor of a broken-parity state for $\tilde{\lambda} > \tilde{\lambda}_c = \sqrt{2\tilde{d}_0 D/V\sigma_c}$. The bifurcation diagram is shown on Fig. 6: it represents the tilt angle ϕ as a function of $\sigma^{-1/2}$, a quantity which is proportional to λ.
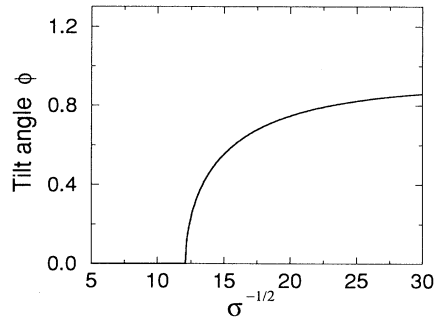
FIG. 6. The bifurcation curve showing the tilt angle as a function of $\sigma^{-1/2}$.

Once we have characterized the parity-breaking transition, we are in a position to analyze the implication on the front undercooling. Expanding Eq. (3.21) up to second order in ϕ, we obtain

$$\Delta = 4\lambda \left[\left[\sigma\theta + \frac{\beta_1}{\pi^3} \right] - \frac{\beta_2}{\pi^2}\phi^2 \right], \qquad (3.26)$$

where β_1 and β_2 result from evaluations of series involved in the calculation ($\beta_1 \simeq 1.0$ and $\beta_2 \simeq 0.12$). For the symmetric state ($\phi = 0$) we recover the Jackson-Hunt result. Using the expression of the tilt angle [Eq. (3.25)], we can evaluate the average front undercooling for asymmetric states. The result is shown in Fig. 7 and compared to the JH branch. The branch associated with the broken-parity states emerges from the JH one at the critical wavelength λ_c, determined above. This branch lies below the JH one, which means that, at fixed wavelength λ ($\lambda > \lambda_c$), broken-parity states have smaller undercooling than the symmetric ones. Equivalently, for a given undercooling the new branch corresponds to faster growth than the JH one. All the features following from Eqs. (3.25) and (3.26) are in qualitative agreement with numerical solution of the full problem [5].

Further results follow. Since the wavelength λ_{min} is often considered as a reference, it is interesting to com-
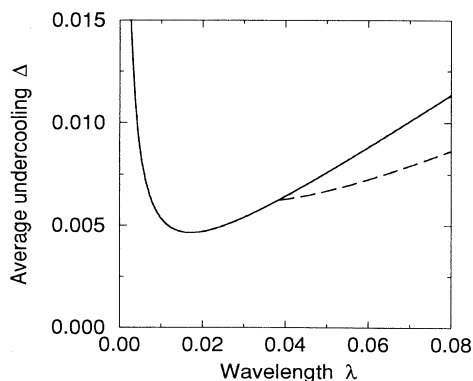
pare the critical wavelength for the onset of parity breaking to it. Using the value of σ_c and the definition of σ [Eq. (3.24)], together with the JH expression of λ_{min}, we obtain

$$\lambda_c / \lambda_{min} \simeq 2.18/\sqrt{\sin(\theta)}. \qquad (3.27)$$

The parity symmetry is lost at wavelength larger than λ_{min}, that is, in a regime where the front dynamics are governed by diffusion, as found from the full numerical analysis. This ratio is plotted in Fig. 8 as a function of the (unique) parameter θ and is compared to the one obtained from the full numerical calculation of the integrodifferential equation (see Ref. [5]). Although our result was expected to be valid at small enough θ, the agreement with the full calculation is impressively good at large angles too. Two remarks are in order. (i) The fact that the JH theory describes well the lower branch for symmetric growth is now well understood and is attributed to the smallness of the Péclet number. Similarly, we could expect our theory, which is adapted to tilted growth to do equally well. (ii) The fact that simple analytic expressions obtained in the small contact angle limit provide good agreement with the full calculation confers to them more importance than what could a priori have been expected. In particular one important result obtained here is the one given by Eq. (3.27). It gives an analytic expression for the appearance of parity breaking, with the minimum undercooling as a reference. In a real experiment the dispersion of wavelength is sometimes large but limited. When the wavelength is large enough, one observes tilted lamellae. Formula (3.27) is a useful expression to confront to experimental findings. Of course, we have in mind that a completely symmetric system is unrealistic and there is a strong need to derive an expression analogous to that given by Eq. (3.27) in the most general case, with the aim to use it in real situations. The calculation, although it involves a tedious algebra, is feasible in principle and we hope to communicate a brief account on this question in the future.

FIG. 7. Undercooling as a function of λ for axisymmetric states (solid line) and broken-parity states (dashed line).
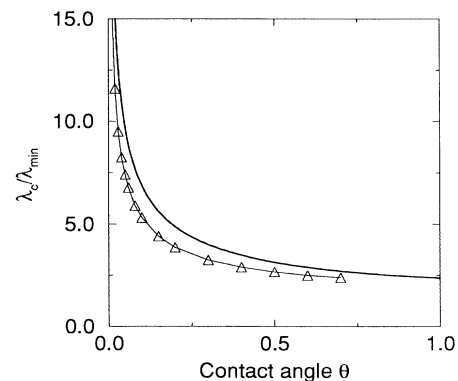

FIG. 8. Ratio of the critical wavelength for the appearance of the broken-parity state to that corresponding to minimum undercooling in the JH theory versus the contact angle in both analytic (triangles) and full numerical (solid line) cases.

B. Off-eutectic compositions

This work is motivated by a belief [14,15] that the deviation from eutectic compositions plays a crucial role in driving some instabilities and in particular the tilting one [15]. Although we found numerically that our result contradicts that of Karma [15] (whose work is based on a random walker method) and that it has been corroborated by recent Monte Carlo simulations [16], it is instructive to see in a transparent way, thanks to the analytic analysis, the role played by off-eutectic compositions.

The novel feature here is the presence of a uniform diffusion boundary layer ahead of the solidification front. We show below that this boundary layer does not play a crucial role in the tilting instability.

For off-eutectic compositions, the two lamellae are not equivalent: they have different widths and consequently different front profiles. (Note that due to mass conservation the volume fraction η of the α phase is related to the melt composition u_∞ [17]. In the small-Péclet-number limit we can safely use $\eta \simeq \frac{1}{2} - u_\infty$.) As a consequence, two consecutive triple points of a broken-parity state are not in general at the same height. So, in order to characterize broken-parity states, we need to introduce another parameter y_0, in addition to the tilt angle ϕ, which measures the height difference between two consecutive triple points. As in Sec. III A, we consider an asymmetric front profile by joining two consecutive triplet points by straight segments:

$$\zeta(x) - \bar{\zeta} = \begin{cases} -\dfrac{y_0}{2} + x \tan(\theta - \phi), & 0 \leq x \leq x_1 \quad (3.28) \\[2mm] \dfrac{y_0}{2} + (\eta\lambda - x)\tan(\theta + \phi), & x_1 \leq x \leq \eta\lambda \quad (3.29) \end{cases}$$

for the α-liquid interface and by

$$\zeta(x) - \bar{\zeta} = \begin{cases} \dfrac{y_0}{2} + (x - \eta\lambda)\tan(\theta - \phi), \\[1mm] \qquad\qquad\qquad \eta\lambda \leq x \leq \eta\lambda + x_2 \quad (3.30) \\[2mm] -\dfrac{y_0}{2} + (\lambda - x)\tan(\theta + \phi), \\[1mm] \qquad\qquad\qquad \eta\lambda + x_2 \leq \lambda \quad (3.31) \end{cases}$$

for the β-liquid interface. The quantities x_1 and $\eta\lambda + x_2$ are the intersection points of the straight segments (see Fig. 9) and are given by

$$x_1 = 2\eta\lambda x_0 + \frac{y_0}{H^{(+)}}, \quad x_2 = 2(1 - \eta\lambda)x_0 - \frac{y_0}{H^{(+)}} . \quad (3.32)$$
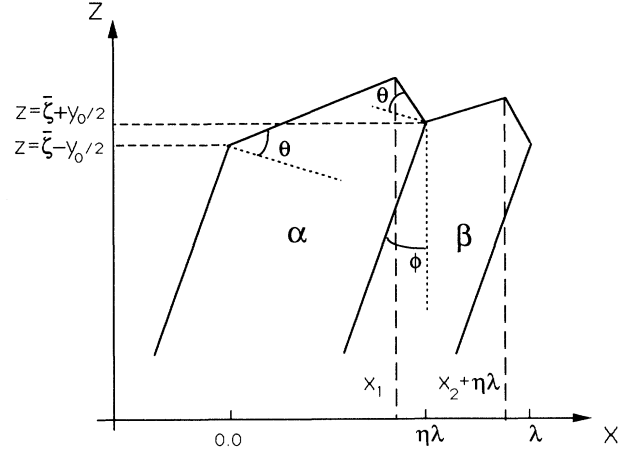

FIG. 9. The front profile used to determine the diffusion field for a nonsymmetric system.

We should remark here that the extent of the α phase is taken in the range $[0, \eta\lambda]$, where η is considered here to have the same value as in the symmetric pattern. It can easily be checked that the correction is $y_0\tan(\phi)$, and we shall see later that at the level of approximation this contribution induces higher-order terms. In fact, we are at liberty to take, in a variational-like formulation, the above profile as the "guessed" one for which we compute the diffusion field and then render the problem self-consistent with that profile. The quantities x_0 and $H^{(+)}$ are the same as those defined in the pure symmetric situation. Note that the triple points sit at a height of $\pm y_0/2$ (measured from the reference position $\bar{\zeta}$). We have made this choice in order to preserve the equivalence between a state characterized by a tilt angle ϕ and a height difference y_0 and the one by a tilt angle $-\phi$ and a height difference $-y_0$. Note also that this front satisfies the mechanical equilibrium conditions [Eqs. (3.4) and (3.5)].

Given this geometry, the strategy is now exactly the same as the one presented above. We determine first the diffusion field corresponding to the front defined above. In the present situation, the expression of the JH field $u^{(0)}$ [Eq. (3.10)] contains an additional term

$$B_0 = \eta - \tfrac{1}{2} , \quad (3.33)$$

which is the strength of the homogeneous diffusion boundary layer. After a heroic boot of algebra, we obtain the expression of the coefficients C_n and write the final result as follows:

$$u(x,z) = u_\infty + F_0 e^{-2(z - \bar{\zeta})} + \sum_{n=1}^{\infty} \left\{ F_n \cos\left[\frac{2\pi n}{\lambda}(x - \eta\lambda/2) \right] - G_n \cos\left[\frac{2\pi n}{\lambda}(x - \eta\lambda/2) \right] \right\} e^{-Q_n(z - \bar{\zeta})} , \quad (3.34)$$

where

$$F_0 = -\frac{y_0}{\lambda}H^{(+)}\tan\phi + (\eta - \tfrac{1}{2})\left\{\frac{\lambda}{H^{(+)}}[\eta^2 + (1-\eta)^2]\tan(\theta+\phi)\tan(\theta-\phi) + \frac{2y_0}{\lambda}\left[(\eta - \tfrac{1}{2})(\lambda - 4x_0) - \frac{2y_0}{H^{(+)}}\right]\right\} + (\eta - \tfrac{1}{2})$$

(3.35)

and

$$F_n = \frac{2\lambda}{\pi^2 n^2}\sin[\eta\pi n] + \frac{\lambda}{2\pi^2 n^2}\tan\phi\{2\sin[\eta\pi n]H^{(-)} + I_n^{(-)}H^{(+)}\}$$

$$+ \frac{2}{\pi n}\sin[\eta\pi n]\left\{\frac{\lambda}{H^{(+)}}[\eta^2 + (1-\eta)^2]\tan(\theta+\phi)\tan(\theta-\phi) - \frac{y_0}{\lambda}\left[(1-2\eta)(\lambda - 4x_0) + \frac{2y_0}{H^{(+)}}\right]\right\}$$

$$+ \frac{\lambda H^{(+)}}{\pi^3 n^3}\sin[\eta\pi n]\cos[\eta\pi n]\{J_n^{(+)} - 2\cos[\eta\pi n]\}$$

$$- \lambda H^{(+)}\sum_{\substack{m=1\\(m\neq n)}}^{\infty}\frac{(m+n)\sin[\eta\pi(m-n)] - (m-n)\sin[\eta\pi(m+n)]}{\pi^3 m^2(m^2 - n^2)}\{J_m^{(+)} - 2\cos[\eta\pi m]\}$$

$$+ 2\lambda H^{(+)}\sum_{m=1}^{n-1}\frac{\sin[\eta\pi(m-n)]}{\pi^3 m^2(m-n)}\{J_m^{(+)} + 2\cos[\eta\pi m]\}\ ,$$

(3.36)

$$G_n = \frac{\lambda}{2\pi^2 n^2}H^{(+)}\tan(\phi)J_n^{(-)} + \frac{\lambda}{\pi^3 n^3}H^{(+)}\sin[\eta\pi n]\cos[\eta\pi n]I_n^{(+)}$$

$$+ \lambda H^{(+)}\sum_{\substack{m=1\\(m\neq n)}}^{\infty}\frac{(m+n)\sin[\eta\pi(m-n)] + (m-n)\sin[\eta\pi(m+n)]}{\pi^3 m^2(m^2 - n^2)}\{I_m^{(+)}\} - 2\lambda H^{(+)}\sum_{m=1}^{n-1}\frac{\sin[\eta\pi(m-n)]}{\pi^3 m^2(m-n)}\{I_m^{(+)}\}\ ,$$

(3.37)

where

$$I_n^{(\pm)} = \sin\left[\frac{2\pi}{\lambda}n(x_2 + \eta\lambda/2)\right]$$

$$\pm\sin\left[\frac{2\pi}{\lambda}n(x_1 - \eta\lambda/2)\right]\ ,$$

(3.38)

$$J_n^{(\pm)} = \cos\left[\frac{2\pi}{\lambda}n(x_2 + \eta\lambda/2)\right]$$

$$\pm\cos\left[\frac{2\pi}{\lambda}n(x_1 - \eta\lambda/2)\right]\ .$$

(3.39)

The coefficients F_n and G_n have the following symmetry properties: $F_n(-\phi, -y_0) = F_n(\phi, y_0)$ and $G_n(-\phi, -y_0) = -G_n(\phi, y_0)$. This can be easily checked by noting that in the transformation $(\phi \to -\phi, y_0 \to -y_0)$, $H^{(\pm)}$ changes into $\pm H^{(\pm)}$, x_0 into $\lambda/2 - x_0$, $(x_1 - \eta\lambda/2)$ into $-(x_1 - \eta\lambda/2)$, and $(x_2 + \eta\lambda/2)$ into $-(x_2 + \eta\lambda/2)$. As in the pure symmetric case, the symmetry properties of the coefficients F_n and G_n are a consequence of the invariance of the diffusion field under the transformation $[\phi \to -\phi, y_0 \to -y_0, x \to -(x - \eta\lambda)]$.

Having obtained the diffusion field we can solve for the front profile, which is compatible with that field. For that purpose, we insert the expression of the diffusion field into the Gibbs-Thomson equation [Eq. (3.15)], which then reads

$$d_0\frac{\zeta_{xx}}{(1 + \zeta_x^2)^{3/2}} + \Delta = \pm u\ (x, z = \bar{\zeta}, \phi, y_0)\ .$$

(3.40)

u is now parametrized by the tilt angle ϕ and the height difference y_0 between two consecutive triple points. Using the mechanical equilibrium conditions at the ends of each lamella [Eqs. (3.4) and (3.5)], we can determine the front profile for each solid-liquid interface, subject to the following additional constraints:

$$\zeta(\eta\lambda, \phi, y_0) - \zeta(0, \phi, y_0) = y_0\ ,$$

(3.41)

$$\zeta(\lambda, \phi, y_0) - \zeta(\eta\lambda, \phi, y_0) = -y_0\ .$$

(3.42)

These two self-consistency equations lead generically to the selection of isolated values of the parameters ϕ and y_0. These two quantities can be thought of as coupled order parameters, which are determined by two minimization-like conditions. In order to exploit the self-consistency equations, we follow the same spirit as that of Sec. III A. The Gibbs-Thomson equation [Eq. (3.40)] can be integrated once over x [from 0 to x ($\leq \eta\lambda$) for the α lamella and from $\eta\lambda$ to x ($\leq \lambda$) for the β lamella]. We obtain

$$\frac{\zeta_x}{\sqrt{1 + \zeta_x^2}} = \sin(\theta - \phi) + \int_0^x \frac{u - \Delta}{d_0}dx \equiv f(x)$$

(3.43)

for the α lamella and

$$\frac{\zeta_x}{\sqrt{1 + \zeta_x^2}} = \sin(\theta - \phi) + \int_{\eta\lambda}^x \frac{u + \Delta}{d_0}dx \equiv g(x)$$

(3.44)

for the β lamella. We then express the slope ζ_x as a function of f for the α-liquid interface and as a function of g for the β-liquid interface, and perform a second integration over each lamella. The result is

$$\zeta(\eta\lambda,\phi,y_0)-\zeta(0,\phi,y_0)=F(\phi,y_0,\lambda,\mu) , \quad (3.45)$$

$$\zeta(\lambda,\phi,y_0)-\zeta(\eta\lambda,\phi,y_0)=G(\phi,y_0,\lambda,\mu) , \quad (3.46)$$

where

$$F(\phi,y_0,\lambda,\mu)=\int_0^{\eta\lambda}\frac{f(x)}{\sqrt{1-f^2}} ,$$

$$G(\phi,y_0,\lambda,\mu)=\int_{\eta\lambda}^{\lambda}\frac{g(x)}{\sqrt{1-g^2}} . \quad (3.47)$$

Here μ is also an abbreviation for the material and control parameters. The self-consistency conditions [Eqs. (3.41) and (3.42)] amount to solving the following nonlinear algebraic equations:

$$F(\phi,y_0,\lambda,\mu)=y_0 , \quad (3.48)$$

$$G(\phi,y_0,\lambda,\mu)=-y_0 . \quad (3.49)$$

These two equations are general expressions for the two unknown quantities ϕ and y_0.

The average front undercooling is easily related to the other parameters λ and μ. It suffices to integrate the Gibbs-Thomson equation over one period. We get

$$\Delta=2(\eta-\tfrac{1}{2})(F_0+u_\infty)+\frac{2d_0}{\lambda}\{\sin(\theta+\phi)+\sin(\theta-\phi)\}$$

$$+2\sum_{n=1}^{\infty}\frac{2\sin[\eta\pi n]}{\pi n}F_n . \quad (3.50)$$

It can be checked that $\Delta(-\phi,-y_0)=\Delta(\phi,y_0)$ (see the symmetry properties of the coefficient F_n). F and G have also a well-defined parity under the transformation $(\phi\to-\phi,y_0\to-y_0)$, $F(-\phi,-y_0)=-F(\phi,y_0)$, and $G(-\phi,-y_0)=-G(\phi,y_0)$. This property is proven in Appendix A. Using the symmetry properties of F and G, we immediately deduce that the self-consistency equations are automatically satisfied for symmetric states ($\phi=0$ and $y_0=0$).

We have to find whether the self-consistency equations are satisfied by nontrivial values of ϕ and y_0. Both equations can be analyzed numerically, but as in the pure symmetric case, we will confine ourselves to the small contact angle limit where the analytic calculation can be pursued to the end. In this limit we can also show (by using the same arguments as before) that f^2 and g^2 can be neglected against 1. This simplification allows us to rewrite the functions F and G as

$$F=\eta\frac{\lambda}{2}\{\sin(\theta-\phi)-\sin(\theta+\phi)\}$$

$$-\sum_{n=1}^{\infty}\frac{\eta\lambda^2}{4d_0\pi n}2\cos[\eta\pi\lambda]G_n$$

$$+\sum_{n=1}^{\infty}\frac{\lambda^2}{4d_0\pi^2 n^2}2\sin[\eta\pi\lambda]G_n , \quad (3.51)$$

$$G=(1-\eta)\frac{\lambda}{2}\{\sin(\theta-\phi)-\sin(\theta+\phi)\}$$

$$+\sum_{n=1}^{\infty}\frac{(1-\eta)\lambda^2}{4d_0\pi n}2\cos[\eta\pi\lambda]G_n$$

$$+\sum_{n=1}^{\infty}\frac{\lambda^2}{4d_0\pi^2 n^2}2\sin[\eta\pi\lambda]G_n . \quad (3.52)$$

We have used in this calculation the expression (3.50) of the undercooling. It is important to note that at this level there is no trace of the uniform boundary layer (i.e., F_0) anymore. At the stage where the functions F and G were defined [see Eq. (3.47)] the term F_0 was still present (in the definition of f) in the bifurcation equation. However, there we had not yet used the expression of the average front undercooling as a function of the other parameters. When we do so, the F_0 terms cancel exactly; the result is expressed by the above two equations. As stated in the Introduction, the homogeneous boundary layer plays a role similar to that of a total net charge, in an analogy with electrostatics. The only terms that survive in the final bifurcation equation are the G_n's. We can mention, if need be, that due to symmetry the homogeneous boundary layer, which is symmetric, does not enter the parity-breaking mechanism. The associated equiconcentration lines are reminiscent of those of a dipolar distribution [18]. Indeed since one phase (the β phase) absorbs, say the B component of the alloy, while the other (the α phase) rejects it, the situation is analogous to that of a distribution of alternating $+$ and $-$ charges. If $\eta=\tfrac{1}{2}$, the total charge is zero and the distribution is purely dipolar, while for $\eta\neq\tfrac{1}{2}$, there is an additional electrostaticlike potential, associated with the homogeneous diffusion boundary layer. The growth mechanism of lamellar eutectics is cooperative and operates on the scale of a wavelength, so that the "electrostatic potential" is ruled out by the local dipole in the mechanism by which a tilted pattern is formed.

In order to analyze the bifurcation, we perform a Taylor expansion of F and G in the small parameters ϕ and y_0. The expansion of F and G up to third order reads

$$F(\phi,y_0)=a_1\phi+c_1y_0+b_1\phi^3+d_1y_0\phi^2+q_1y_0^2\phi+p_1y_0^3 , \quad (3.53)$$

$$G(\phi,y_0)=a_2\phi+c_2y_0+b_2\phi^3+d_2y_0\phi^2+q_2y_0^2\phi+p_2y_0^3 , \quad (3.54)$$

where the coefficients a_i, b_i, c_i, d_i, p_i, and q_i are functions of the wavelength λ and the volume fraction η of the α phase. Their expressions are given by

$$a_1(\lambda,\eta)=\eta\pi R_1+S_1-4\eta\pi^4\sigma ,$$

$$a_2(\lambda,\eta)=-(1-\eta)\pi R_1+S_1-4(1-\eta)\pi^4\sigma ,$$

$$b_1(\lambda,\eta)=\pi^2(\eta\pi R_2+S_2)/6\theta^2 ,$$

$$b_2(\lambda,\eta)=\pi^2[-(1-\eta)\pi R_2+S_2]/6\theta^2 ,$$

$$c_1(\lambda,\eta)=\eta\pi S_3+R_3 ,$$

$$c_2(\lambda,\eta)=-(1-\eta)\pi S_3+R_3 . \quad (3.55)$$

R_1, S_1, R_2, S_2, R_3, and S_3 are numerical series depending on the value of the parameter η (their explicit expressions are given in Appendix B). The series S_i are even functions of the parameter $(\eta - \frac{1}{2})$ while the series R_i are odd functions of the same parameter. The coefficients d_i, p_i, and q_i will not enter the subsequent calculation, as we shall see below, so that we do not give their expressions. Note that the expansions (3.53) and (3.54) are composed only of those terms which are compatible with the symmetries evoked above.

Let us focus on the expansion of the function F and our reasoning will apply perfectly well to the function G. Our aim is to extract from the first bifurcation equation $(F = y_0)$ y_0 as a function of ϕ, which upon substitution in the second equation $(G = -y_0)$ provides the expression of ϕ. First it can be checked with the help of definitions (3.55) and Appendix B (where the series S's and R's are defined) that for $\eta = \frac{1}{2}$, we have $a_1 = a_2$ and $b_1 = b_2$. A substraction of Eqs. (3.53) and (3.54) provides $y_0 = 0$, and when substituting this result into both equations we obtain two identical results, which are nothing but the bifurcation equation in the completely symmetric system. If we confine our attention to small deviations from the symmetric system, it is legitimate to keep only the leading term in y_0 in Eqs. (3.53) and (3.54). On the other hand, a_1 is small close to the critical point (by continuity from the symmetric case), so that ϕ^3 should be kept in the determination of y_0 as a function of ϕ (in the reference state where $\eta = \frac{1}{2}$, $\phi^3 \sim a_1 \phi$). We can thus reduce Eqs. (3.53) and (3.54) to the following expressions:

$$F(\phi, y_0) = a_1\phi + c_1 y_0 + b_1\phi^3 + (\text{higher-order terms}) ,$$
$$\tag{3.56}$$

$$G(\phi, y_0) = a_2\phi + c_2 y_0 + b_2\phi^3 + (\text{higher-order terms}) .$$
$$\tag{3.57}$$

From the first self-consistency equation $(F = y_0)$, we obtain an expression of y_0 as a function of ϕ

$$y_0 = \frac{a_1}{1 - c_1}\phi + \frac{b_1}{1 - c_1}\phi^3 .$$
$$\tag{3.58}$$

Plugging this expression into the second self-consistency equation $(G = -y_0)$, we obtain a closed expression for the tilt angle ϕ

$$a\phi + b\phi^3 = 0 ,$$
$$\tag{3.59}$$

where

$$a = a_2(1 - c_1) + a_1(1 - c_2) = -8\pi^8\sigma^2 + 4\pi^4 T\sigma + U ,$$
$$\tag{3.60}$$

$$b = b_2(1 - c_1) + b_1(1 - c_2) = (4\pi^4 V\sigma + W)\frac{\pi^2}{6\theta^2} ,$$
$$\tag{3.61}$$

with

$$T = (\eta - \tfrac{1}{2})\pi R_1 + S_1 + (1 - \eta)\eta\pi S_3 - (\eta - \tfrac{1}{2})R_3 ,$$

$$U = \pi(R_1 R_3 - S_1 S_3)/2 ,$$

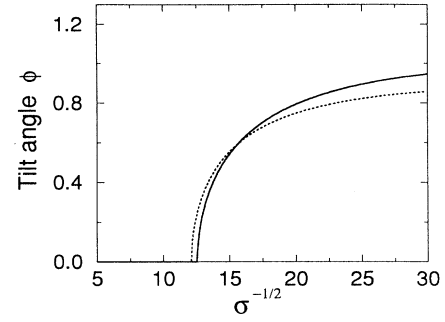$$V = (\eta - \tfrac{1}{2})\pi R_2 + S_2 , \quad W = R_2 R_3 - S_2 S_3 .$$

FIG. 10. The bifurcation curve showing the tilt angle as a function of $\sigma^{-1/2}$ for $\eta = 0.4$ (full line) and for $\eta = 0.5$ (dotted line), i.e., for a symmetric system.

A numerical examination of a and b show that b is always positive while a changes sign for a critical value σ_c of σ given by

$$\sigma_c = (T + \sqrt{T^2 + \pi U}\,)/4\pi^2 .$$
$$\tag{3.62}$$

We find that for $\sigma > \sigma_c$ there exists only the trivial solution $\phi = 0$ while for $\sigma < \sigma_c$, the initially symmetric state undergoes a transition to the broken-parity state characterized by a nonzero value of ϕ. We show in Fig. 10 the bifurcation curves for different values of η (i.e., different values of the melt composition). They exhibit exactly the same features as in the purely symmetric case $(\eta = \frac{1}{2})$. The only difference is that the critical wavelength is increased when we move away from the eutectic composition. We show in Fig. 11 the variation of the critical wavelength as function of η. For $\eta = 0.65$ (or equivalently $\eta = 0.35$) the critical wavelength is 10% larger than in the purely symmetric case.

We can also expand the average front undercooling up to the second order
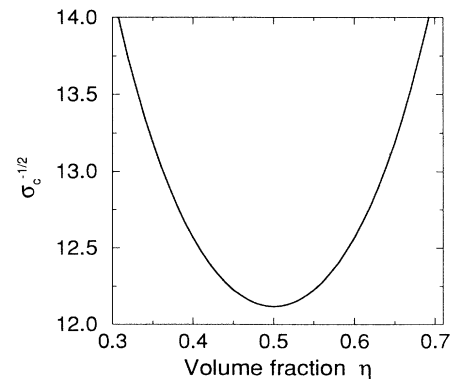
$$\Delta = c - d\phi^2 ,$$
$$\tag{3.63}$$

where

FIG. 11. Variation of the critical value $\sigma_c^{-1/2}$ as a function of the volume fraction η.
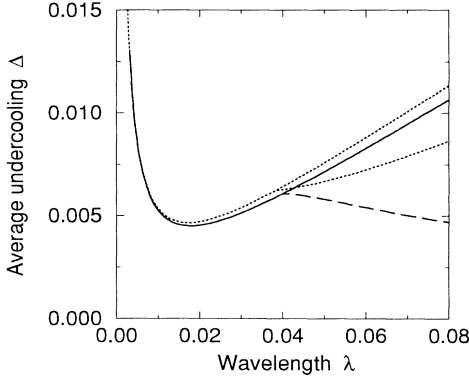
FIG. 12. Undercooling as a function of λ for axisymmetric states (solid line) and broken-parity states (dashed line) for a nonsymmetric system ($\eta=0.4$). We compare it with that obtained for a symmetric system ($\eta=0.5$) (dotted lines).

$$c =4\lambda \left[\sigma\theta+\frac{S_4}{\pi^3}\right], \quad d =4\lambda \left[\frac{S_5}{\pi^2}-\frac{S_4}{\pi^3}\right] . \qquad (3.64)$$

S_4 and S_5 are numerical series whose values depend on η. They are even functions of $(\eta-\frac{1}{2})$ (see Appendix B). We observe the same feature as in the pure symmetric case ($\eta=\frac{1}{2}$). Figure 12 shows that the more we move away from the eutectic composition, the larger the reduction in the front undercooling in comparison with the JH result. This result may explain that it is easier to create tilted domains with off-eutectic compositions than with eutectic ones.

IV. CRYSTALLINE ANISOTROPY

It has been known for a long time that lamellar eutectics are generally composed of eutectic grains, i.e., domains with uniform crystal orientations of the two eutectic phases. The following question therefore arises: Are there correlations between crystal and lamellar orientations and if so what is their strength? Experimental observations [19] show that within a grain the basic state, i.e., the pattern which in the absence of anisotropy is made of straight lamellae parallel to the growth direction, is generally tilted with a small but definite angle ($\leq 5°$). This small tilting of the basic state has been interpreted as an effect of the weak anisotropy of the surface energies. This interpretation has been supported by a perturbative analytic calculation in the small contact angle limit [19]. Another important question naturally arises: How does the parity-breaking transition manifest itself since the basic state is in general already weakly tilted? The broken-parity state, which results from a dynamical instability, is characterized by a rather large tilt angle (about 20°). So the transition, we are interested in is that between weakly and strongly tilted states. In lamellar growth experiments, it seems difficult, starting with a given grain, to produce stable strongly tilted domains with tilt angle of both signs, as to be expected for a true symmetry-breaking transition. In general, the

lamellar structure preferentially tilts in one direction and not in the opposite one. The preferential direction corresponds generally to that of the basic state. This observation has found a natural explanation in anisotropy [20]. This question was addressed only phenomenologically or solved numerically [21]. Our purpose here is to account analytically for the effect of anisotropy on the parity-breaking transition starting from the "microscopic" equations. We will first introduce the changes that are needed to account for crystalline anisotropy. Then we will follow exactly the same spirit as used in the purely isotropic case to analyze the influence of anisotropy on the parity-breaking transition. Since it has been found that the homogeneous diffusion layer is not crucial for parity breaking, we shall confine ourselves to the eutectic composition case.

In the presence of crystalline anisotropy the appropriate physical quantity is not the interface tension γ, but the interface stiffness $\gamma+\gamma''$ (where the prime designates the derivative with respect to the polar angle). If the surface tension is written as

$$\gamma_{ik} =\gamma_{ik}^{(0)}\{1+\tilde{a}_{ik}\cos[4(\vartheta-\theta_a)]\} , \qquad (4.1)$$

it immediately follows that the capillary length takes the form

$$d =d_0\{1-\epsilon\cos[4(\vartheta-\theta_a)]\} \qquad (4.2)$$

with

$$\epsilon \equiv 15\tilde{a}_{sl}, \quad d_0 =\frac{\gamma_{sl}^{(0)}T_e}{m_l L \Delta c} .$$

ϑ is defined as the angle between the z direction and the normal to the interface. Finally θ_a is the angle defining the crystal orientation with the z axis as a reference (ϑ and θ_a are measured with the trigonometric convention). We consider that the strengths of anisotropies and the direction of the crystal direction of the minimum energy are the same for each γ_{ij}, so that they are all characterized by a single strength ϵ and a single angle θ_a. This does not alter the general conclusion which we shall draw here.

A consequence of crystalline anisotropy is that the mechanical equilibrium conditions have to be reformulated. Indeed the interfaces are now subject, besides the surface-tension force, to torques whose contributions are proportional to γ'_{ik}. The equilibrium at the triple points then takes the form

$$\Gamma_{\alpha l}+\Gamma_{\beta l}+\Gamma_{\alpha\beta}=0 , \qquad (4.3)$$

where the vectors Γ_{ik} are no longer parallel with the phase interfaces; $\Gamma_{ik}\equiv\|\Gamma_{ik}\|=[\gamma_{ik}^2+\gamma_{ik}'^2]^{1/2}$ and the angle between Γ_{ik} and γ_{ik} is given by $\Delta_{ik}=\arctan(\gamma'_{ik}/\gamma_{ik})$. The contact angles θ_α and θ_β (see Fig. 13) can be determined by this vector equation. Equation (4.3) can be projected along the direction parallel to $\Gamma_{\alpha\beta}$ and perpendicular to it to provide

$$-\Gamma_{\alpha l}(-\tilde{\theta}_\alpha)\cos(\psi_\alpha)+\Gamma_{\beta l}(\tilde{\theta}_\beta)\cos(\psi_\beta)=0 , \qquad (4.4)$$

$$\Gamma_{\alpha l}(-\tilde{\theta}_\alpha)\sin(\psi_\alpha)+\Gamma_{\beta l}(\tilde{\theta}_\beta)\sin(\psi_\beta)=\Gamma_{\alpha\beta}(\phi) , \qquad (4.5)$$
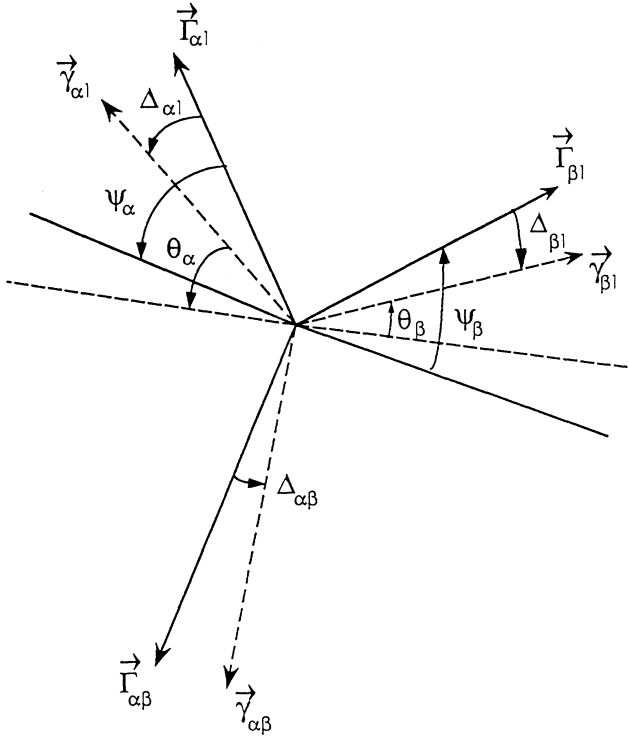
FIG. 13. Scheme representing the vectors γ_{ik} and Γ_{ik} at the α-β triple point. The vectors γ_{ik} are parallel with the phase interfaces while the vectors Γ_{ik} are not. The contact angle θ_α (θ_β) is defined as the angle between γ_{al} ($\gamma_{\beta l}$) and the perpendicular to $\gamma_{\alpha\beta}$. ψ_α (ψ_β) measure the angle between Γ_{al} ($\Gamma_{\beta l}$) and the perpendicular to $\Gamma_{\alpha\beta}$. Note that the orientation of these angles has been chosen so that they are positive with respect to the trigonometric orientation. Finally the quantities Δ_{ik} represent the angles between Γ_{ik} and γ_{ik}.

where

$$\tilde{\theta}_\alpha = \theta_\alpha + \phi , \qquad (4.6)$$

$$\tilde{\theta}_\beta = \theta_\beta - \phi . \qquad (4.7)$$

The angles ψ_α and ψ_β (see Fig. 13) are simply related to the contact angles θ_α and θ_β by

$$\psi_\alpha = \theta_\alpha + \Delta_{al} - \Delta_{\alpha\beta} , \qquad (4.8)$$

$$\psi_\beta = \theta_\beta - \Delta_{\beta l} + \Delta_{\alpha\beta} . \qquad (4.9)$$

The quantities Γ_{ik} depend on the interface orientation. The pinning angles $\tilde{\theta}_\alpha$ and $\tilde{\theta}_\beta$ define the orientation of the α-liquid and the β-liquid interface, respectively, while the tilt angle ϕ determines the orientation of α-β interface. Note that these equations have been written for the α-β triple points. The equations for the β-α triple points are identical since the α and β lamellae are supposed to have exactly the same physical properties.

We shall assume here a weak enough anisotropy, so that a first-order expansion about the isotropic case makes sense. Within this context, the contact angles take the form

$$\theta_\alpha = \theta^{(0)} + \epsilon s_\alpha(\theta^{(0)}, \phi) , \qquad (4.10)$$

$$\theta_\beta = \theta^{(0)} + \epsilon s_\beta(\theta^{(0)}, \phi) . \qquad (4.11)$$

s_α and s_β are functions of the contact angle $\theta^{(0)}$ and the tilt angle ϕ (see Appendix C). We use the superscript (0) to recall that we refer to the isotropic case.

For a tilted pattern, with an angle ϕ, the pinning angles $\tilde{\theta}$ and $\tilde{\theta}'$ at the two ends of a given lamella are simply given by

$$\tilde{\theta} = \theta_\beta - \phi , \qquad (4.12)$$

$$\tilde{\theta}' = \theta_\alpha + \phi . \qquad (4.13)$$

Now we are prepared to deal with the coupling between the spontaneous parity-breaking transition and crystalline anisotropy. The diffusion field is obviously given by the same expression as in the isotropic case [Eq. (3.12)]. The only difference now is that since our profile to compute this field is chosen in a such way that it is compatible with mechanical equilibrium, the definitions of some parameters in the front profile will be altered to take this into account. More precisely the coefficients D_n and E_n are deduced from those calculated in the pure isotropic case [Eqs. (3.13) and (3.14)] by replacing $\theta^{(0)} + \phi$ by $\theta_\alpha + \phi$ and $\theta^{(0)} - \phi$ by $\theta_\beta - \phi$. The only quantities that are involved in this change are $H^{(\pm)}$ and x_0, which should be redefined as

$$H^{(\pm)} = \tan(\theta_\alpha + \phi) \pm \tan(\theta_\beta - \phi) , \qquad (4.14)$$

$$x_0 = \frac{\lambda \tan(\theta_\alpha + \phi)}{2H^{(+)}} . \qquad (4.15)$$

The new field should now satisfy the Gibbs-Thomson condition, which takes the form

$$d_0 \{ 1 - \epsilon \cos[4(\vartheta - \theta_a)] \} \frac{\zeta_{xx}}{(1 + \zeta_x^2)^{3/2}} + \Delta$$

$$= \pm u (x, z = \bar{\zeta}, \phi) , \qquad (4.16)$$

with the profile subject to the constraint $\zeta(\lambda/2, \phi) - \zeta(0, \phi) = 0$.

We follow exactly step by step the same procedure as for the isotropic problem. It is still possible to find a first integral of Eq. (4.16), which provides the slope ζ_x as a function of the other parameters. However, since the expression obtained did not allow us to go further into the analytic analysis, we shall here directly use the approximation of small contact angles, as used before, but still keep the term which is responsible for the destruction of the pitchfork bifurcation. The small contact angle limit amounts to neglecting higher-order terms in ζ_x in Eq. (4.16). It follows that Eq. (4.16) takes to leading order in ζ_x the following form:

$$d_0 \{ 1 - \epsilon[\cos(4\theta_a) + 4\sin(4\theta_u)\zeta_x] \} \zeta_{xx} + \Delta$$

$$= \pm u (x, z = \bar{\zeta}, \phi) . \qquad (4.17)$$

A first integration yields

$$\zeta_x - \epsilon[\cos(4\theta_a)\zeta_x + 2\sin(4\theta_a)\zeta_x^2] = f , \qquad (4.18)$$

where

$$f \equiv \tan(\theta_\beta - \phi) - \epsilon[\cos(4\theta_a)\tan(\theta_\beta - \phi)$$
$$+ 2\sin(\theta_a)\tan^2(\theta_\beta - \phi)]$$
$$+ \int_0^x \frac{u - \Delta}{d_0} dx \ . \tag{4.19}$$

It is useful to split f into two parts; the isotropic and the anisotropic one. We set

$$f = f^{(0)} + \epsilon f^{(1)} \ , \tag{4.20}$$

where $f^{(0)}$ is the isotropic part of f while $f^{(1)}$ is the leading-order contribution coming from anisotropy. Their expressions are simply given by

$$f^{(0)} = \tan(\theta^{(0)} - \phi) + \int_0^x \frac{u^{(0)} - \Delta^{(0)}}{d_0} dx \ , \tag{4.21}$$

$$f^{(1)} = -[\cos(4\theta_a)\tan(\theta^{(0)} - \phi)$$
$$+ 2\sin(4\theta_a)\tan^2(\theta^{(0)} - \phi)]$$
$$+ \frac{s_\beta}{\cos^2(\theta^{(0)} - \phi)} + \int_0^x \frac{u^{(1)} - \Delta^{(1)}}{d_0} dx \ , \tag{4.22}$$

where $u = u^{(0)} + \epsilon u^{(1)}$ and $\Delta = \Delta^{(0)} + \epsilon\Delta^{(1)}$, and use has been made of $\theta_\beta = \theta^{(0)} + \epsilon s_\beta$ [see Eq. (4.10)]. $u^{(0)}$ and $\Delta^{(0)}$ are the diffusion field and the average undercooling obtained in the absence of anisotropy, while $u^{(1)}$ is the first-order term obtained by expansion of the actual field and $\Delta^{(1)}$ is the corresponding first-order deviation of the front undercooling, which we shall derive below as a function of the other parameters.

Now we need to get an expression for ζ, on which to impose the self-consistency condition. In the isotropic case we have $\zeta_x = f^{(0)}$, so that to leading order Eq. (4.17) can be written as

$$\zeta_x = f^{(0)} + \epsilon[\cos(4\theta_a)f^{(0)} + f^{(1)}] \ , \tag{4.23}$$

which is easily integrated. The self-consistency condition then becomes

$$F(\phi, \lambda, \mu) \equiv \int_0^{\lambda/2} \{f^{(0)} + \epsilon[\cos(4\theta_a)f^{(0)} + f^{(1)}]\}dx$$
$$= 0 \ , \tag{4.24}$$

where μ stands for the control and material parameters. This equation is a general expression for the parameter ϕ as a function of the other parameters. The undercooling is given by $\Delta = \Delta^{(0)} + \epsilon\Delta^{(1)}$ with

$$\Delta^{(0)} = \frac{2d_0}{\lambda}[\tan(\theta^{(0)} + \phi) + \tan(\theta^{(0)} - \phi)]$$
$$+ 2\sum_{n=1}^\infty \frac{D_{2n-1}^{(0)}}{\pi(2n-1)} \ , \tag{4.25}$$

$$\Delta^{(1)} = -\frac{2d_0}{\lambda}\{\cos(4\theta_a)[\tan(\theta^{(0)} + \phi) + \tan(\theta^{(0)} - \phi)]$$
$$+ 2\sin(4\theta_a)[\tan^2(\theta^{(0)} + \phi) - \tan^2(\theta^{(0)} - \phi)]\}$$
$$+ \frac{2d_0}{\lambda}\left\{\frac{s_\alpha}{\cos^2(\theta^{(0)} + \phi)} + \frac{s_\beta}{\cos^2(\theta^{(0)} - \phi)}\right\}$$
$$+ 2\sum_{n=1}^\infty \frac{D_{2n-1}^{(1)}}{\pi(2n-1)} \ . \tag{4.26}$$

Using these expressions, we can write the function F [Eq. (4.24)] as

$$F = \frac{\lambda}{4}[\tan(\theta^{(0)} - \phi) - \tan(\theta^{(0)} + \phi)]\frac{\lambda^2}{2\pi d_0}\sum_{n(>0)}\frac{E_{2n-1}^{(0)}}{(2n-1)^2}$$

$$+ \epsilon\left\{\frac{\lambda}{2}\sin(4\theta_a)[\tan^2(\theta^{(0)} - \phi) + \tan^2(\theta^{(0)} + \phi)] + \frac{\lambda}{4}\left[\frac{s_\beta}{\cos^2(\theta^{(0)} - \phi)} - \frac{s_\alpha}{\cos^2(\theta^{(0)} + \phi)}\right]\right.$$

$$\left. + \frac{\lambda^2}{2\pi d_0}\sum_{n(>0)}\frac{\cos(4\theta_a)E_{2n-1}^{(0)} + E_{2n-1}^{(1)}}{(2n-1)^2}\right\} \ . \tag{4.27}$$

If $\epsilon = 0$, we recover the result we obtained in the absence of anisotropy. The new contribution (the terms in ϵ) expresses the effect of anisotropy.

We can now make an expansion of F in ϕ. We expand the isotropic terms up to the third order in ϕ while we just take (in a perturbative scheme) the leading term ($\phi = 0$) in ϕ of the anisotropic terms. The result is

$$\pi^4(\sigma_c - \sigma)\phi - \frac{\alpha_2}{4\theta^{(0)2}}\phi^3 + \epsilon v = 0 \ , \tag{4.28}$$

with

$$v = \frac{\pi^4}{2}\{(s_{\alpha 0} - s_{\beta 0})(\sigma_c - \sigma) - 4\theta^{(0)2}\sin(4\theta_a)\sigma\} \ , \tag{4.29}$$

where $\sigma_c = \alpha_1/\pi^4$ ($\alpha_1 = 0.66$), $\alpha_2 = 2.95$, and $s_{\alpha 0, \beta 0} = s_{\alpha,\beta}(\theta^{(0)}, \phi = 0)$. If $\epsilon = 0$, we recover immediately the result found in the isotropic case. The anisotropy yields an homogeneous term v in the bifurcation equation (4.29). In the range of wavelength we are interested in (i.e., where λ is close to the critical value λ_c corresponding to the parity-breaking bifurcation point in the ab-
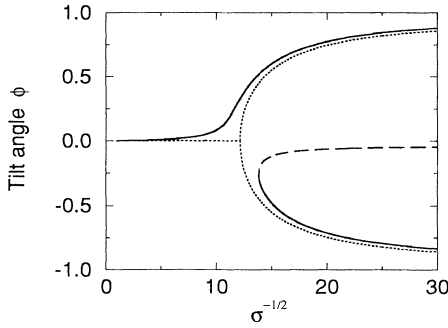
FIG. 14. The bifurcation diagram of the tilt angle as a function of $\sigma^{-1/2}$ for anisotropic surface tension ($\epsilon=0.5$ and $\theta_a=-0.1$). Stable branches are represented by solid lines and unstable ones by dashed lines. The dotted lines represent the bifurcation diagram for isotropic surface tension ($\epsilon=0$).

sence of anisotropy), v has a well-defined sign which is given by the orientation of the crystalline anisotropy [$v=-2\pi^4\theta^{(0)^2}\sin(\theta_\alpha)\sigma_c$]. The main effect due to the presence of this homogeneous term is to render the bifurcation imperfect.

Figure 14 shows the behavior of the tilt angle ϕ as a function of σ. The dashed part represents the unstable branch. This problem is similar, for example, to that of a ferromagnetic transition (where ϕ plays the role of magnetization) in an external applied magnetic field [which plays a similar role as the v term in Eq. (3.23)]. The bifurcation equation (4.28) was postulated in a previous paper [21].

V. CONCLUSION

This paper has dealt with a successful analytic theory of parity breaking in lamellar eutectic growth. Our analysis is very simple in its spirit (although not as simple in the algebra) but captures the main essential features.

To emphasize the basic ingredients of parity breaking we did not want to unnecessarily make the presentation too complex, and therefore we first restricted ourselves to a situation where the solid phases have the same physical properties. This had the advantage to greatly simplify the algebra. The confrontation of the present results with those obtained in our previous complete (and sophisticated) numerical work has shown that there is a good quantitative agreement between the two treatments. Our analytic formulas can be used with confidence in real situations.

In a second part we have shown in a transparent way how the homogeneous diffusion boundary layer—which is related to off-eutectic compositions—is not crucial in the mechanism by which tilted pattern is formed (it simply enters in mass conservation on the global scale). Its nonrelevance is now beyond any doubt.

The third line of this work has dealt with the effect of crystalline anisotropy, an effect which is persistent in real experiments. We have shown from the "microscopic" model that crystalline anisotropy destroys the pitchfork bifurcation in favor of an imperfect one.

Finally, we keep naturally in mind that we should extend our calculation to the most general case where the two solid phases have different properties. This should provide us with analytic expressions—such as the wavelength at which parity breaking takes place as a function of the physical parameters—which should be crucial to guide further experimental developments.

APPENDIX A: DETERMINATION OF THE PARITY OF F AND G

We would like to check the symmetry properties of the functions $F(\phi,y_0)$ and $G(\phi,y_0)$ involved in the analytic treatment of parity breaking for melt at off-eutectic composition (in the absence of anisotropy). Of course the following proof also applies to the function F calculated in the particular case where the melt is at eutectic composition.

First we focus on the function $F(\phi,y_0)$. We consider the quantity $F(-\phi,-y_0)$, which is given by

$$F(-\phi,-y_0)=\int_0^{\eta\lambda}\frac{f(x,-\phi,-y_0)}{\sqrt{1+f^2(x,-\phi,-y_0)}}dx , \tag{A1}$$

with

$$f(x,-\phi,-y_0)$$
$$=\sin(\theta+\phi)$$
$$+\int_0^x\frac{u(X,-\phi,-y_0)-\Delta(-\phi,-y_0)}{d_0}dX . \tag{A2}$$

Let $Y=\eta\lambda-X$ in the expression of $f(x,-\phi,-y_0)$. This change of variable transforms Eq. (A2) into

$$f(x,-\phi,-y_0)=\sin(\theta+\phi)$$
$$-\int_{\eta\lambda}^{\eta\lambda-x}\frac{(Y,\phi,y_0)-\Delta(\phi,y_0)}{d_0}dY , \tag{A3}$$

where we have used the symmetry properties of the diffusion field and that of the average front undercooling. Namely, we have $u(X,-\phi,-y_0)=u(Y,\phi,y_0)$ and $\Delta(-\phi,-y_0)=\Delta(\phi,y_0)$.

The procedure now consists in splitting the integral appearing in Eq. (A3) into two parts as follows:

$$f(x,-\phi,-y_0)=\sin(\theta+\phi)$$
$$-\int_{\eta\lambda}^0\frac{u(Y,\phi,y_0)-\Delta(\phi,y_0)}{d_0}dY$$
$$-\int_0^{\eta\lambda-x}\frac{u(Y,\phi,y_0)-\Delta(\phi,y_0)}{d_0}dY . \tag{A4}$$

The first integral can easily be evaluated by using the Gibbs-Thomson relation for the α phase ($d_0\kappa = u - \Delta$). The result is $\sin(\theta - \phi) + \sin(\theta + \phi)$. Then we can rewrite (A4) as

$$f(x, -\phi, -y_0)$$
$$= -\sin(\theta - \phi) - \int_0^{\eta\lambda - x} \frac{u(Y, \phi, y_0) - \Delta(\phi, y_0)}{d_0} dY$$
$$= -f(\eta\lambda - x, \phi, y_0) . \tag{A5}$$

It suffices now to insert this relation into Eq. (A1), and by making the last change of variable $X = \eta\lambda - x$, we obtain the desired symmetry property

$$F(-\phi, -y_0) = -\int_0^{\eta\lambda} \frac{f(\eta\lambda - x, \phi, y_0)}{\sqrt{1 + f^2(\eta\lambda - x, \phi, y_0)}} dx$$
$$= -\int_0^{\eta\lambda} \frac{f(X, \phi, y_0)}{\sqrt{1 + f^2(X, \phi, y_0)}} dX$$
$$= -F(\phi, y_0) . \tag{A6}$$

By following the same strategy as that exposed above we can also easily check the symmetry property of the function $G(\phi, y_0)$.

APPENDIX B: EXPRESSIONS OF THE SERIES R_i AND S_i

In this appendix we give the expressions of the series R_i and S_i ($i = 1, 2, 3$) involved in the expansion of the functions $F(\phi, y_0)$ and $G(\phi, y_0)$. We will also give the expressions of the series S_4 and S_5 appearing in the expansion of the undercooling $\Delta(\phi, y_0)$.

We first define four quantities which will be useful in the following. These quantities are

$$a_{n,m} = 2[1 + \cos(2\eta\pi n)]\sin(\eta\pi m) , \tag{B1}$$

$$b_{n,m} = 2\sin(2\eta\pi n)\cos(\eta\pi m) , \tag{B2}$$

$$c_{n,m} = 2\sin(2\eta\pi n)\sin(\eta\pi m) , \tag{B3}$$

$$d_{n,m} = 2[1 - \cos(2\eta\pi n)]\cos(\eta\pi m) . \tag{B4}$$

The series R_1 and S_1 can be written in the following form:

$$R_1 = -R_1^1 + 2R_1^2 - 2R_1^3 , \tag{B5}$$

$$S_1 = S_1^1 - 2S_1^2 + 2S_1^3 , \tag{B6}$$

where

$$R_1^1 = \sum_{n=1}^{\infty} \frac{\eta + (-1)^n(1-\eta)}{n^3}\{4\sin(\eta\pi n)\cos^2(\eta\pi n)\} , \tag{B7}$$

$$R_1^2 = \sum_{n=1}^{\infty} \sum_{m=1}^{n-1} \frac{\eta + (-1)^m(1-\eta)}{nm(m-n)}\{a_{n,m} - b_{n,m}\} , \tag{B8}$$

$$R_1^3 = \sum_{n=1}^{\infty} \sum_{\substack{m=1 \\ (m \neq n)}}^{\infty} \frac{\eta + (-1)^m(1-\eta)}{nm(m^2 - n^2)}\{ma_{n,m} - nb_{n,m}\} , \tag{B9}$$

and

$$S_1^1 = \sum_{n=1}^{\infty} \frac{\eta + (-1)^n(1-\eta)}{n^4}\{4\sin^2(\eta\pi n)\cos(\eta\pi n)\} , \tag{B10}$$

$$S_1^2 = \sum_{n=1}^{\infty} \sum_{m=1}^{n-1} \frac{\eta + (-1)^m(1-\eta)}{n^2 m(m-n)}\{c_{n,m} - d_{n,m}\} , \tag{B11}$$

$$S_1^3 = \sum_{n=1}^{\infty} \sum_{\substack{m=1 \\ (m \neq n)}}^{\infty} \frac{\eta + (-1)^m(1-\eta)}{n^2 m(m^2 - n^2)}\{mc_{n,m} - nd_{n,m}\} , \tag{B12}$$

while S_2 and R_2 can be expressed as

$$R_2 = R_2^1 - 2R_2^2 + 2R_2^3 , \tag{B13}$$

$$S_2 = -S_2^1 + 2S_2^2 - 2S_2^3 , \tag{B14}$$

where

$$R_2^1 = \sum_{n=1}^{\infty} \frac{\eta^3 + (-1)^n(1-\eta)^3}{n}\{4\sin(\eta\pi n)\cos^2(\eta\pi n)\} , \tag{B15}$$

$$R_2^2 = \sum_{n=1}^{\infty} \sum_{m=1}^{n-1} \frac{m[\eta^3 + (-1)^m(1-\eta)^3]}{n(m-n)}\{a_{n,m} - b_{n,m}\} , \tag{B16}$$

$$R_2^3 = \sum_{n=1}^{\infty} \sum_{\substack{m=1 \\ (m \neq n)}}^{\infty} \frac{m[\eta^3 + (-1)^m(1-\eta)^3]}{n(m^2 - n^2)}\{ma_{n,m} - nb_{n,m}\} , \tag{B17}$$

and

$$S_2^1 = \sum_{n=1}^{\infty} \frac{\eta^3 + (-1)^n(1-\eta)^3}{n}\{4\sin^2(\eta\pi n)\cos(\eta\pi n)\} , \tag{B18}$$

$$S_2^2 = \sum_{n=1}^{\infty} \sum_{m=1}^{n-1} \frac{m[\eta^3 + (-1)^m(1-\eta)^3]}{n^2(m-n)}\{c_{n,m} - d_{n,m}\} , \tag{B19}$$

$$S_2^3 = \sum_{n=1}^{\infty} \sum_{\substack{m=1 \\ (m \neq n)}}^{\infty} \frac{m[\eta + (-1)^m(1-\eta)^3]}{n^2(m^2 - n^2)}\{mc_{n,m} - nd_{n,m}\} . \tag{B20}$$

Finally S_3 and R_3 are given by

$$R_3 = R_3^1 - 2R_3^2 + 2R_3^3 , \tag{B21}$$

$$S_3 = -S_3^1 + 2S_3^2 - 2S_3^3 , \tag{B22}$$

where

$$R_3^1 = \sum_{n=1}^{\infty} \frac{\eta - (-1)^n(1-\eta)}{n^4} \{4\sin^2(\eta\pi n)\cos(\eta\pi n)\} \ ,$$

(B23)

$$R_3^2 = \sum_{n=1}^{\infty} \sum_{m=1}^{n-1} \frac{\eta - (-1)^m(1-\eta)}{n^2 m(m-n)} \{c_{n,m} - d_{n,m}\} \ ,$$ (B24)

$$R_3^3 = \sum_{n=1}^{\infty} \sum_{\substack{m=1 \\ (m \neq n)}}^{\infty} \frac{\eta - (-1)^m(1-\eta)}{n^2 m(m^2 - n^2)} \{m c_{n,m} - n d_{n,m}\} \ ,$$

(B25)

$$S_3^1 = \sum_{n=1}^{\infty} \frac{\eta(-1)^n(1-\eta)}{n^3} \{4\sin(\eta\pi n)\cos^2(\eta\pi n)\} \ ,$$

(B26)

$$S_3^2 = \sum_{n=1}^{\infty} \sum_{m=1}^{n-1} \frac{m[\eta - (-1)^m(1-\eta)]}{nm(m-n)} \{a_{n,m} - b_{n,m}\} \ ,$$

(B27)

$$S_3^3 = \sum_{n=1}^{\infty} \sum_{\substack{m=1 \\ (m \neq n)}}^{\infty} \frac{m[\eta - (-1)^m(1-\eta)]}{nm(m^2 - n^2)} \{m a_{n,m} - n b_{n,m}\} \ .$$

(B28)

The series S_4 and S_5 appearing in the expansion of $\Delta(\phi, y_0)$ are found to be

$$S_4 = \sum_{n=1}^{\infty} \frac{\sin^2(\eta\pi n)}{n^3} \ ,$$ (B29)

$$S_5 = \sum_{n=1}^{\infty} \frac{\eta - (-1)^n(1-\eta)}{n^2} \sin(\eta\pi n) \ .$$ (B30)

We can note that the series S_i are even functions of the variable $(\eta - \frac{1}{2})$ while the series R_i are odd functions of this variable. As a consequence, $R_i(\eta = \frac{1}{2}) = 0$.

APPENDIX C:
DERIVATION OF THE EXPRESSION
OF THE CONTACT ANGLES
IN THE WEAK ANISOTROPY LIMIT

We would like here to derive the expressions of the contact angles θ_α and θ_β in the limit where the anisotropy of surface energies is weak. Our starting point is the set of equations (4.4) and (4.5) which expresses the mechanical equilibrium condition at the triple points. The strategy consists in expanding these equations up to first order in the small parameter ϵ (which measures the strength of anisotropy). By setting

$$\Gamma_{ik} = \Gamma_{ik}^{(0)} + \epsilon\Gamma_{ik}^{(1)} \ ,$$ (C1)

$$\psi_\alpha = \psi_\alpha^{(0)} + \epsilon\psi_\alpha^{(1)} \ ,$$ (C2)

$$\psi_\beta = \psi_\beta^{(0)} + \epsilon\psi_\beta^{(1)}$$ (C3)

(where i and k denote α, β, or l), Eqs. (4.4) and (4.5) can be rewritten as

$$-[\Gamma_{\alpha l}^{(0)} + \epsilon\Gamma_{\alpha l}^{(1)}][\cos(\psi_\alpha^{(0)}) - \epsilon\psi_\alpha^{(1)}\sin(\psi_\alpha^{(0)})]$$

$$+[\Gamma_{\beta l}^{(0)} + \epsilon\Gamma_{\beta l}^{(1)}][\cos(\psi_\beta^{(0)}) - \epsilon\psi_\beta^{(1)}\sin(\psi_\beta^{(0)})] = 0 \ ,$$ (C4)

$$[\Gamma_{\alpha l}^{(0)} + \epsilon\Gamma_{\alpha l}^{(1)}][\sin(\psi_\alpha^{(0)}) + \epsilon\psi_\alpha^{(1)}\cos(\psi_\alpha^{(0)})]$$

$$+[\Gamma_{\beta l}^{(0)} + \epsilon\Gamma_{\beta l}^{(1)}][\sin(\psi_\beta^{(0)}) + \epsilon\psi_\beta^{(1)}\cos(\psi_\beta^{(0)})]$$

$$= \Gamma_{\alpha\beta}^{(0)} + \epsilon\Gamma_{\alpha\beta}^{(1)} \ .$$ (C5)

We recall that the angles ψ_α and ψ_β (see Fig. 13) are simply related to the contact angles θ_α and θ_β by

$$\psi_\alpha^{(0,1)} = \theta_\alpha^{(0,1)} + \Delta_{\alpha l}^{(0,1)} - \Delta_{\alpha\beta}^{(0,1)} \ ,$$ (C6)

$$\psi_\beta^{(0,1)} = \theta_\beta^{(0,1)} - \Delta_{\beta l}^{(0,1)} + \Delta_{\alpha\beta}^{(0,1)} \ .$$ (C7)

Using the definition of the quantities Γ_{ik} ($\Gamma_{ik} = [\gamma_{ik}^2 + \gamma_{ik}'^2]^{1/2}$), together with the expression of surface tensions γ_{ik} [Eq. (4.1)] we can determine the zeroth- and first-order contribution of the Γ_{ik}'s. We find

$$\Gamma_{\alpha l}^{(0)} = \gamma_{sl}^{(0)}, \quad \Gamma_{\alpha l}^{(1)} = \gamma_{sl}^{(0)}\cos[-4(\theta_\alpha^{(0)} + \phi + \theta_a)] \ ,$$

$$\Gamma_{\beta l}^{(0)} = \gamma_{sl}^{(0)}, \quad \Gamma_{\beta l}^{(1)} = \gamma_{sl}^{(0)}\cos[4(\theta_\beta^{(0)} - \phi - \theta_a)] \ ,$$ (C8)

$$\Gamma_{\alpha\beta}^{(0)} = \gamma_{\alpha\beta}^{(0)}, \quad \Gamma_{\alpha\beta}^{(1)} = \gamma_{\alpha\beta}^{(0)}\cos[-4(\phi + \theta_a)] \ .$$

We can equally derive the expressions of the angles Δ_{ik} to zeroth and first order in ϵ by using the fact that $\Delta_{ik} = \arctan(\gamma_{ik}'/\gamma_{ik})$. The result is

$$\Delta_{\alpha l}^{(0)} = 0, \quad \Delta_{\alpha l}^{(1)} = -4\sin[-4(\theta_\alpha^{(0)} + \phi + \theta_a)] \ ,$$

$$\Delta_{\beta l}^{(0)} = 0, \quad \Delta_{\beta l}^{(1)} = -4\sin[4(\theta_\beta^{(0)} - \phi - \theta_a)] \ ,$$ (C9)

$$\Delta_{\alpha\beta}^{(0)} = 0, \quad \Delta_{\alpha\beta}^{(1)} = -4\sin[-4(\phi + \theta_a)] \ .$$

Our aim now is to determine the expressions of $\psi_\alpha^{(0,1)}$ and $\psi_\beta^{(0,1)}$ from Eqs. (C4) and (C5) and then to plug them into (C6) and (C7) in order to obtain the expressions of the contact angles $\theta_\alpha^{(0,1)}, \theta_\beta^{(0,1)}$.

To order ϵ^0, the two equations (C4) and (C5) give

$$-\Gamma_{sl}^{(0)}\cos(\psi_\alpha^{(0)}) + \Gamma_{sl}^{(0)}\cos(\psi_\beta^{(0)}) = 0 \ ,$$ (C10)

$$\Gamma_{sl}^{(0)}\sin(\psi_\alpha^{(0)}) + \Gamma_{sl}^{(0)}\sin(\psi_\beta^{(0)}) = \Gamma_{\alpha\beta}^{(0)} \ .$$ (C11)

We recover the result found in the isotropic case. We have $\psi_\alpha^{(0)} = \psi_\beta^{(0)} \equiv \theta^{(0)}$ (where $\sin\theta^{(0)} = \Gamma_{\alpha\beta}^{(0)}/\Gamma_{sl}^{(0)}$), so that $\theta_\alpha^{(0)} = \theta_\beta^{(0)} = \theta^{(0)}$.

To order ϵ the set of equations (C4) and (C5) yields

$$[\Gamma_{sl}^{(0)}\psi_\alpha^{(1)} - \Gamma_{sl}^{(0)}\psi_\beta^{(1)}]\sin\theta^{(0)} = [\Gamma_{\alpha l}^{(1)} - \Gamma_{\beta l}^{(1)}]\cos\theta^{(0)} \ ,$$ (C12)

$$[\Gamma_{sl}^{(0)}\psi_\alpha^{(1)} + \Gamma_{sl}^{(0)}\psi_\beta^{(1)}]\cos\theta^{(0)}$$

$$= \Gamma_{\alpha\beta}^{(1)} - [\Gamma_{\alpha l}^{(1)} + \Gamma_{\beta l}^{(1)}]\sin\theta^{(0)} \ .$$ (C13)

Note that use has been made of the fact that $\psi_\alpha^{(0)} = \psi_\beta^{(0)} \equiv \theta^{(0)}$. Solving this set of equations we obtain

$$\psi_\alpha^{(1)} = \frac{1}{\sin[2\theta^{(0)}]} \{\cos[2\theta^{(0)}]\cos[4(\theta^{(0)} + \phi + \phi_a)]$$

$$-\cos[4(\theta^{(0)} - \phi - \theta_a)]$$

$$+\sin^2[\theta^{(0)}]\cos[4(\phi + \theta_a)]\} \ ,$$ (C14)

$$\psi_\beta^{(1)} = \frac{1}{\sin[2\theta^{(0)}]}\{\cos[2\theta^{(0)}]\cos[4(\theta^{(0)}-\phi-\theta_a)]$$

$$-\cos[4(\theta^{(0)}+\phi+\theta_a)]$$

$$+\sin^2[\theta^{(0)}]\cos[4(\phi+\theta_a)]\} , \quad (C15)$$

where we have made use of the expressions of the $\Gamma_{ik}^{(1)}$'s [Eq. (C8)].

Finally we can determine the expressions of $\theta_\alpha^{(1)}$ and $\theta_\beta^{(1)}$ by using Eqs. (C6) and (C7), together with the expressions of the $\Delta_{ik}^{(1)}$'s [Eq. (C9)]. The result is

$$\theta_\alpha^{(1)} = \psi_\alpha^{(1)} - 4\{\sin[4(\theta^{(0)}+\phi+\theta_a)]-\sin[4(\phi+\theta_a)]\} , \quad (C16)$$

$$\theta_\beta^{(1)} = \psi_\alpha^{(1)} - 4\{\sin[4(\theta^{(0)}-\phi-\theta_a)]+\sin[4(\phi+\theta_a)]\} . \quad (C17)$$

In summary we can write

$$\theta_\alpha = \theta^{(0)} + \epsilon s_\alpha(\theta^{(0)},\phi,\theta_a) ,$$

$$\theta_\beta = \theta^{(0)} + \epsilon s_\beta(\theta^{(0)},\phi,\theta_a) , \quad (C18)$$

where s_α and s_β are given by Eqs. (C16) and (C17), as functions of $\theta^{(0)}$, ϕ, and θ_a [by using the expressions of $\psi_{\alpha,\beta}^{(1)}$ given by Eqs. (C14) and (C15)].

The quantity of interest is the difference $s_{\alpha 0}-s_{\beta 0}$ evaluated at $\phi=0$ (it appears in the bifurcation equation). From the above equations we find that

$$s_{\alpha 0} - s_{\beta 0} = \frac{\cos[\theta^{(0)}]}{\sin[\theta^{(0)}]}\{\cos[4(\theta^{(0)}+\theta_a)]-\cos[4(\theta^{(0)}-\theta_a)]\} + 8\sin[4\theta_a] + 4\{\sin[4(\theta^{(0)}-\theta_a)]-\sin[4(\theta^{(0)}+\theta_a)]\} , \quad (C19)$$

and in the small contact angle limit we simply have

$$s_{\alpha 0} - s_{\beta 0} = -8\sin(4\theta_a) . \quad (C20)$$

*Also at Groupe de Physique des Solides, Universités Paris 7 et 6, 2 Place Jussieu, 75 005, Paris, France.

†Present address: Laboratoire de Physique de l'ENS de Lyon, 46 Allée d'Italie 69000 Lyon, France. Permanent address: I. P. Bardin Institute for Ferrous Metals, Moscow 107005, Russia.

[1] K. A. Jackson and J. D. Hunt, Trans. Metall. Soc. AIME 236, 1129 (1966).

[2] J. S. Langer, Phys. Rev. Lett. 44, 1023 (1980).

[3] Klaus Kassner, Alexandre Valance, Chaouqi Misbah, and Dmitrii Temkin, Phys. Rev. E (to be published).

[4] K. Kassner and C. Misbah, Phys. Rev. A 44, 6513 (1991).

[5] K. Kassner and C. Misbah, Phys. Rev. A 44, 6533 (1991).

[6] A. J. Simon, J. Bechhoefer, and A. Libchaber, Phys. Rev. Lett. 63, 2574 (1988).

[7] C. Faivre, S. de Cheveigné, C. Guthmann, and P. Kurowski, Europhys. Lett. 9, 779 (1989).

[8] M. Rabaud, S. Michalland, and Y. Couder, Phys. Rev. Lett. 64, 184 (1990).

[9] K. Kassner and C. Misbah, Phys. Rev. Lett. 65, 1458 (1990); 66, 522(E) (1991).

[10] H. Levine and W. J. Rappel, Phys. Rev. A 42, 7475 (1990).

[11] C. Misbah and D. E. Temkin, Phys. Rev. A 46, R4497 (1992).

[12] H. Levine, W. J. Rappel, and H. Riecke, Phys. Rev. A 43, 1122 (1991).

[13] Chaouqi Misbah and Alexandre Valance (unpublished).

[14] V. Datye and J. S. Langer, Phys. Rev. B 24, 4155 (1981).

[15] A. Karma, Phys. Rev. Lett. 59, 71 (1987).

[16] Rong-Fu Xiao, J. Iwan D. Alexander, and Franz Rosenberger (unpublished).

[17] K. Kassner and C. Misbah, J. Phys. A 25, 3213 (1992).

[18] C. Misbah and H. Müller-Krumbaar (unpublished).

[19] B. Caroli, C. Caroli, G. Faivre, and J. Mergy, J. Cryst. Growth 118, 135 (1992).

[20] G. Faivre and J. Mergy, Phys. Rev. A 45, 7320 (1992).

[21] K. Kassner and C. Misbah, Phys. Rev. A 45, 7372 (1992).